Chapter 6

Time-Variant Robustness of Aging Structures

Fabio Biondini
Department of Civil and Environmental Engineering, Politecnico di Milano, Milan, Italy

Dan M. Frangopol
Department of Civil and Environmental Engineering, Lehigh University, Bethlehem, Pennsylvania, USA

Abstract

This chapter presents recent advances in the field of structural robustness and progressive collapse of deteriorating structural systems, with emphasis on the relationships among structural robustness, static indeterminacy, structural redundancy, and failure times. Damage is viewed as a progressive deterioration of the material properties and its amount is evaluated at the member level by means of a damage index associated with prescribed patterns of cross-sectional deterioration. The variation of suitable performance indicators compared with the amount of damage is used to formulate dimensionless measures of structural robustness. An index of structural integrity is defined to quantify the severity of the structural failure with respect to its consequences. The role of damage propagation on structural robustness is investigated by considering different propagation mechanisms and by using a damage-sensitive fault-tree analysis. The role of structural robustness on progressive collapse, as well as the relationship between structural robustness and static indeterminacy, are also investigated by considering parallel and mixed series-parallel truss deteriorating systems with various degrees of static indeterminacy. Time-variant measures of structural robustness and redundancy are developed with respect to the loads associated to the first local failure and to the structural collapse. The elapsed time between these two types of failures is investigated as a measure of the ability of the system to be repaired after local failure. This approach is illustrated through the application to a reinforced concrete frame under different corrosion damage scenarios.

Keywords

Aging, corrosion, deterioration, diffusion, failure times, life-cycle performance, static indeterminacy, structural lifetime, structural redundancy, structural robustness.

6.1 Introduction

During the last few decades, progressively increasing attention has been focused on the concept of structural robustness, disproportionate failure and progressive collapse. The first developments in this field followed the partial collapse in 1968 of the Ronan Point high rise building in London after a relatively small and localized gas explosion (Griffiths et al. 1968). More recently, other building collapse events – including the

DOI: 10.1201/b17073-7
http://dx.doi.org/10.1201/b17073-7

terrorist attacks to the Alfred P. Murrah Federal Building in Oklahoma City in 1995 and the Twin Towers at the World Trade Center in New York in 2001 – emphasized the need for additional research towards the development of new concepts and methods in this field (Carper & Smilowitz 2006).

As a consequence of these and other dramatic structural failures, the importance of reliable design procedures leading to conceive robust structures has been emphasized over the years and it is widely recognized (Taylor 1975, Ellingwood & Leyendecker 1978, Ellingwood & Dusenberry 2005, Starossek 2009). This is not limited to buildings, but it is also recognized as a major concern for progressive collapse of bridges (Starossek 2008). However, in structural design the concept of robust structures, or damage-tolerant structures, is still an issue of controversy. Actually, despite the fact that procedures aimed to identify weak links within structures have been reported in literature (see for example Lu et al. 1999, Agarwal et al. 2003) and efforts have been made to quantify robustness based on risks due to failure consequences (Baker et al. 2008), there are no well established or generally accepted criteria for a consistent definition and a quantitative measure of structural robustness (Starossek & Haberland 2011).

Another crucial aspect not clarified yet is the relationship amongst structural robustness and structural redundancy. In fact, the terms robustness and redundancy are often used as synonymous. However, they denote different properties of the structural system. Structural robustness can be viewed as the ability of the system to suffer an amount of damage not disproportionate with respect to the causes of the damage itself. Structural redundancy can instead be defined as the ability of the system to redistribute among its members the load which can no longer be sustained by some other damaged members. Redundancy is usually associated with the degree of static indeterminacy. However, it has been demonstrated that the degree of static indeterminacy is not a consistent measure for structural redundancy. In fact, structural redundancy depends on many factors, such as structural topology, member sizes, material properties, applied loads and load sequence, among others (Frangopol & Curley 1987, Frangopol & Klisinski 1989, Frangopol & Nakib 1991).

In addition, robustness and redundancy evaluations are usually related to damage suddenly provoked by accidental actions, such as explosions or impacts (Ellingwood 2006, Ghosn et al. 2010, Saydam & Frangopol 2011, 2013). However, damage could also arise gradually in time from aging of structures (Biondini et al. 2004, 2006, Ellingwood 2005). Damage propagation mechanisms may also involve disproportionate effects and alternate load redistribution paths (Biondini & Restelli 2008, Biondini 2009, Okasha & Frangopol 2010a, Decò et al. 2011). These effects are particularly relevant for concrete buildings and bridges exposed to corrosion and other kinds of environmental damage. Notable events of bridge collapses due to the environmental aggressiveness and related phenomena, such as corrosion and fatigue, include for example the Silver Bridge in 1967 (ASCE 1968), and the Mianus River Bridge in 1983 (NTSB 1983). Therefore, it is of great interest to develop suitable life-cycle measures of structural robustness with respect to a progressive deterioration of the structural performance.

Structural systems under progressive damage have been investigated to identify suitable measures for structural redundancy (Frangopol & Curley 1987, Frangopol et al. 1992) and structural robustness (Biondini & Restelli 2008). More recently, the time

factor has been explicitly included in a lifetime scale for a time-variant measure of structural robustness (Biondini 2009, Biondini & Frangopol 2010a) and structural redundancy (Okasha & Frangopol 2010a, Decò et al. 2011). Advances have also been accomplished to identify the local failure modes and to evaluate their occurrence in time to maintain a suitable level of performance of deteriorating systems and to avoid the structural collapse over the lifetime (Biondini & Frangopol 2010b, Biondini 2012). In fact, repairable local failures can be considered as a warning of possible occurrence of more severe and not repairable failures.

The aim of this chapter is to present the latest research findings in the field of structural robustness and progressive collapse of deteriorating structural systems, with emphasis on the relationship among structural robustness, static indeterminacy, structural redundancy, and failure times. In the presented approaches, damage is viewed as a progressive deterioration of the material properties and its amount is evaluated at the member level by means of a damage index associated with prescribed patterns of cross-sectional deterioration. The deterioration effects on the system performance are evaluated with reference to suitable performance indicators identified with parameters of the structural response. The variation of these indicators with respect to the values associated with the performance of the undamaged system is compared with the amount of damage to formulate dimensionless measures of structural robustness. Moreover, an index of structural integrity is defined to quantify the severity of the structural failure with respect to its consequences.

The role of damage propagation on structural robustness is then investigated by considering different propagation mechanisms and by using a damage-sensitive fault-tree analysis. In such a way, all the feasible damage paths associated with the propagation mechanism and the actual topology of the system are described by branched networks where the level of activation of each nodal connection is properly tuned to account for the prescribed amount of local structural damage. The role of structural robustness on progressive collapse as well as the relationship between structural robustness and static indeterminacy are also investigated by considering parallel and series-parallel truss deteriorating systems with various degrees of static indeterminacy.

Finally, these general criteria are applied to concrete structures exposed to corrosion. The effects of the damage process on the structural performance are evaluated by using a proper methodology for life-cycle assessment of concrete structures exposed to diffusive attacks from environmental aggressive agents. Time-variant measures of structural robustness and redundancy are developed with respect to the loads associated to the first local failure and to the structural collapse. The elapsed time between these two types of failures is investigated as a measure of the ability of the system to be repaired after local failure. This approach is illustrated using a reinforced concrete (RC) frame under different corrosion damage scenarios.

6.2 Damage Modeling

Deterioration processes are generally complex and their effects and evolution over time depend on both the damage mechanism and type of materials and structures. For steel structures the main causes of lifetime deterioration are corrosion and fatigue. For concrete structures there is a wider spectrum of aging and damage mechanisms that may seriously affect the life-cycle performance. These mechanisms include chemical

processes associated to sulfate and chloride attacks and alkali-silica reactions, physical processes due to freeze/thaw cycles and thermal cycles, and mechanical processes such as cracking, abrasion, erosion, and fatigue (Ellingwood 2005). Deterioration models could be developed on empirical bases, as it is generally necessary for rate-controlled damage processes, or founded on mathematical descriptions of the underlying physical mechanisms, as it is often feasible for diffusion-controlled damage processes.

6.2.1 *Deterioration Patterns*

A mathematical description of deterioration processes may be complex and not always feasible due to lack of information and incomplete knowledge of the damage mechanisms. However, effective models can often be established for practical applications by assuming the structural damage as a progressive deterioration of the material properties. According to this approach, the amount of deterioration is specified at the member level by means of time-variant damage indices $\delta = \delta(t) \in [0; 1]$ associated with prescribed patterns of deterioration, with $\delta = 0$ and $\delta = 1$ for the undamaged and fully damaged states, respectively (Frangopol & Curley 1987, Biondini & Restelli 2008).

Several damage mechanisms, including uniform corrosion in steel structures, as well as crushing, cracking, abrasion and erosion in concrete structures, can be effectively represented at the member level by a progressive reduction of the effective resistant area of the member cross-section. As an example, for hollowed circular cross-sections having internal and external radius r_i and r_e, respectively, and damaged along an external layer of uniform thickness Δr, the amount of damage can be specified by means of the following damage index:

$$\delta = \frac{\Delta r}{r_e - r_i} \tag{6.1}$$

In this way, proper correlation laws may be introduced to define the variation of the geometrical properties of the cross-section, such as area A and moment of inertia I, as a function of the damage index δ. Figure 6.1 shows the variation of the area ratio $\alpha = \alpha(\delta) = A/A_0$ for two circular cross-sections, ① solid and ② hollowed, undergoing uniform damage along the external boundary (Biondini & Restelli 2008).

Different patterns of deterioration are needed when localized damage occurs. This is the case of corrosion in concrete structures where damage starts to develop locally in the reinforcing steel bars and propagates affecting both the corroded steel bars and the surrounding volume of concrete. By denoting p the corrosion penetration depth, the damage index δ for reinforcing steel bars could be defined as follows:

$$\delta = \frac{p}{D_0} \tag{6.2}$$

where D_0 is the diameter of the undamaged steel bar. The corresponding percentage loss $\delta_s = \delta_s(\delta) = 1 - A_s/A_{s0}$ of steel resistant area A_s for a corroded reinforcement bar depends on the corrosion mechanism. In carbonated concrete without relevant chloride content, corrosion tends to develop uniformly on the steel bars along an external layer of thickness Δr, with $p = 2\Delta r$ and $\delta_s = \delta(2 - \delta)$. In the presence of chlorides, corrosion

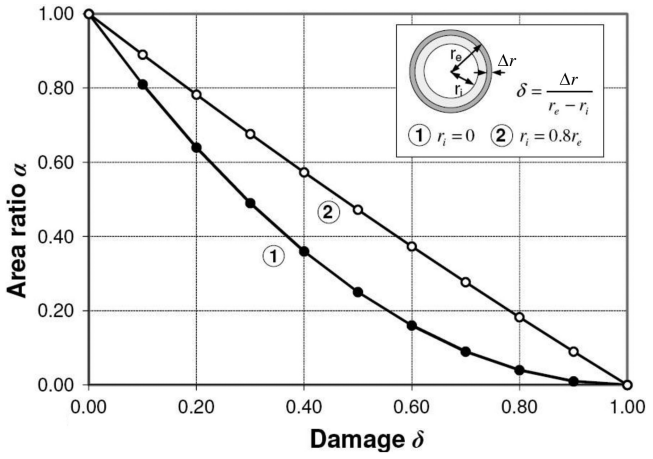

Figure 6.1 Area ratio $\alpha = A/A_0$ versus damage index δ for circular cross-sections, ① solid and ② hollowed, undergoing uniform damage along the external boundary (adapted from Biondini & Restelli 2008).

tends instead to localize (pitting corrosion), and the relationship $\delta_s = \delta_s(\delta)$ depends on the shape of the pit (Stewart 2009).

This study will focus on the effects of corrosion in terms of mass loss of the reinforcing steel bars. A general formulation of damage modeling for uniform and pitting corrosion involving reduction of cross-sectional area of corroded bars, reduction of steel ductility, deterioration of concrete strength, and spalling of concrete cover, can be found elsewhere (Biondini 2011).

6.2.2 *Deterioration Rate*

The evolution over time of the deterioration process needs to be described by suitable models of time-variant deterioration rate. Simple empirical models are often adopted, for example (Ellingwood 2005):

$$\delta(t) = \kappa(t - t_i)^{\eta} \tag{6.3}$$

where t_i is the initiation time and κ and η are parameters determined from regression of available data. Empirical models are amenable to an efficient implementation in life-cycle prediction frameworks. Moreover, they often represent the only feasible approach to model rate-controlled damage processes. On the other hand, it is worth noting that the parameters of these empirical models are sensitive to several factors that characterize the problem and, in most cases, such sensitivity does not allow for a generalization to situations that are not covered by the available database. For this reason, when possible, more complex and comprehensive mathematical models are developed to represent the actual deterioration mechanisms and their effects on the life-cycle structural performance.

A mathematical description of time-variant deterioration may be feasible for diffusion-controlled damage processes, where the deterioration rate generally depends on the concentration of the diffusive agents. This is the typical case of concrete structures, where damage induced by the diffusive attack of aggressive agents, such as sulfates and chlorides, may involve deterioration of concrete and corrosion of reinforcement (CEB 1992, Bertolini et al. 2004). The diffusion process can be effectively described by using the Fick's laws which, in the case of a single component diffusion in isotropic, homogeneous and time-invariant media, can be reduced to the following second order partial differential linear equation (Glicksman 2000):

$$D\nabla^2 C = \frac{\partial C}{\partial t} \tag{6.4}$$

where D is the diffusivity coefficient of the medium, $C = C(\mathbf{x}, t)$ is the concentration of the chemical component at point $\mathbf{x} = \mathbf{x}(x, y, z)$ and time t, $\nabla C = \mathbf{grad}\ C(\mathbf{x}, t)$ and $\nabla^2 = \nabla \cdot \nabla$.

In such processes, damage induced by mechanical loading interacts with the environmental factors and accelerates both diffusion and deterioration. Therefore, the dependence of the deterioration rate on the concentration of the diffusive agent is generally very complex, and the available information about environmental factors and material characteristics is usually not sufficient for a detailed modeling. However, despite such complexities and drawbacks, simple degradation models may be often successfully adopted for an overall evaluation of the life-cycle structural performance (Biondini et al. 2004, 2006, Biondini & Frangopol 2008, 2009). In particular, a linear dependency can be approximately assumed between the rate of damage and the concentration of the aggressive agent (Biondini et al. 2004):

$$\frac{\partial \delta_s(\mathbf{x}_m, t)}{\partial t} = \frac{C(\mathbf{x}_m, t)}{C_s \Delta t_s}, \quad t \geq t_{im} \tag{6.5}$$

where $\delta_{sm} = \delta_s(\mathbf{x}_m, t)$ is the damage index of the mth reinforcement bar located at point $\mathbf{x}_m = (y_m, z_m)$ over a concrete cross-section, C_s is the value of constant concentration $C(\mathbf{x}_m, t)$ which would lead to a complete damage of the steel bar over the time interval Δt_s, $t_{im} = \max\{t \mid C(\mathbf{x}_m, t) \leq C_{cr}\}$ is the corrosion initiation time, and C_{cr} is a critical threshold of concentration. On the basis of available data for sulfate and chloride attacks (Pastore & Pedeferri 1994) and correlations between chloride content and corrosion current density in concrete (Bertolini et al. 2004, Liu & Weyers 1998, Thoft-Christensen 1998) a linear relationship between rate of corrosion in the range 0–200 mm/year and chloride content in the range 0–3% could be reasonable for RC structures exposed to severe environmental conditions.

6.2.3 *Local and Global Measures of Damage*

A damage index $\delta = \delta(\mathbf{x}, t)$ provides a comprehensive description of the spatial distribution of damage over the structure. However, due to its *local* nature, it is not useful for global evaluations of system robustness. A synthetic *global* measure of damage

$\Delta = \Delta(t)$ can be derived by a weighted average over the structural volume V as follows (Biondini 2004):

$$\Delta(t) = \frac{\int_V w(\mathbf{x}, t)\delta(\mathbf{x}, t)dV}{\int_V w(\mathbf{x}, t)dV} \tag{6.6}$$

where $w = w(\mathbf{x}, t)$ is a suitable weight function. This formulation can be applied to corrosion of reinforcing steel bars of concrete members as follows (Biondini 2009):

$$\Delta(t) = \frac{\sum_m w_m(t)\delta_{sm}(t)A_{s0m}}{\sum_m w_m(t)A_{s0m}} \tag{6.7}$$

and extended at the structural level by a weighted integration over all members of the system. Arithmetic average with constant weights functions $w(\mathbf{x}, t) = w_m(t) = w_0$ can be adopted if there are no portions of material volume or reinforcing steel bars playing a specific role in the damage process.

6.3 Structural Performance Indicators

Strength and ductility, as well as other performance indicators of the ultimate conditions under nonlinear behavior, may be used in robustness evaluations associated with damage induced by severe loadings, such as explosions or impacts (Frangopol & Curley 1987, Biondini et al. 2008, Biondini & Frangopol 2010a, 2013). However, performance indicators of the serviceability conditions under linear behavior, such as elastic stiffness and first yielding strength, may become of major importance in life-cycle robustness evaluations associated with aging of structures (Biondini & Restelli 2008). In addition, it has been noted that the assumption of linear behavior can be successfully used in design of robust structures (Powell 2009). Therefore, in the following several performance indicators under both linear elastic and nonlinear behavior are investigated.

6.3.1 *Parameters of Structural Behavior*

The following parameters related to the structural behavior of linear systems are considered:

$$d = \det(\mathbf{K}) \tag{6.8}$$

$$\tau = \sum_i \vartheta_i(\mathbf{K}) \tag{6.9}$$

$$c = \frac{\max_i \vartheta_i(\mathbf{K})}{\min_i \vartheta_i(\mathbf{K})} \tag{6.10}$$

$$T_n = 2\pi\sqrt{\max_i \vartheta_i(\mathbf{K}^{-1}\mathbf{M})} \tag{6.11}$$

where d, τ, and c are, respectively, the determinant, the trace, and the condition number of the stiffness matrix $\mathbf{K}$, T_n is the first natural vibration period associated with the mass matrix $\mathbf{M}$, and $\vartheta_i(\mathbf{A})$ denotes the ith eigenvalue of a square matrix $\mathbf{A}$.

These performance indicators are of wide generality, since they are related to the properties of the structural system only. However, a structural system may have different performance under different loads. For this reason, the following indicators associated with a prescribed loading condition are also considered:

$$s = \|\mathbf{s}\| = \|\mathbf{K}^{-1}\mathbf{f}\| \tag{6.12}$$

$$\Phi = \frac{1}{2}\mathbf{s}^T\mathbf{K}\mathbf{s} = \frac{1}{2}\mathbf{s}^T\mathbf{f} \tag{6.13}$$

where $\mathbf{s}$ is the displacement vector, $\mathbf{f}$ is the applied load vector, Φ is the stored energy, and $\|\cdot\|$ denotes the Euclidean scalar norm. These indicators depend on both the system properties and the loading condition.

The performance indicators defined in Equations (6.8) to (6.13) may refer either to the system in the original state, in which the structure is fully intact, or to the system in a perturbed state, in which a prescribed damage scenario is applied. However, for robustness evaluations it is also of interest to define indicators able to simultaneously account for the structural performance of the intact system and of the damaged system.

6.3.2 *Pseudo-Loads*

To define indicators able to simultaneously account for the structural performance of both the intact and damaged systems, it is useful to consider the following linear equilibrium equations:

$$\mathbf{K}_0\mathbf{s}_0 = \mathbf{f}_0 \tag{6.14}$$

$$\mathbf{K}_1\mathbf{s}_1 = \mathbf{f}_1 \tag{6.15}$$

where the subscripts "0" and "1" refer to the intact state and the damaged state of the structure, respectively (Figure 6.2a). Based on these equations, the displacement vector of the intact system $\mathbf{s}_0$ can be related to the displacement vector of the damaged system $\mathbf{s}_1$ as follows:

$$\mathbf{s}_0 = \mathbf{s}_1 + \mathbf{K}_1^{-1}\hat{\mathbf{f}}_1 = \mathbf{K}_1^{-1}(\mathbf{f}_1 + \hat{\mathbf{f}}_1) \tag{6.16}$$

$$\hat{\mathbf{f}}_1 = (\mathbf{K}_1 - \mathbf{K}_0)\mathbf{s}_0 - (\mathbf{f}_1 - \mathbf{f}_0) = \Delta\mathbf{K}\mathbf{s}_0 - \Delta\mathbf{f} \tag{6.17}$$

where $\hat{\mathbf{f}}_1$ is a vector of nodal forces equivalent to the effects of repair (Figure 6.2b). This vector represents the additional nodal forces that must be applied to the damaged system to achieve the nodal displacements of the intact system, and it is called *backward pseudo-load vector* (Biondini & Restelli 2008). As an example, Figure 6.3 shows the backward pseudo-loads for a frame system undergoing deterioration of one column according to the damage model shown in Figure 6.1 for cross-section ①.

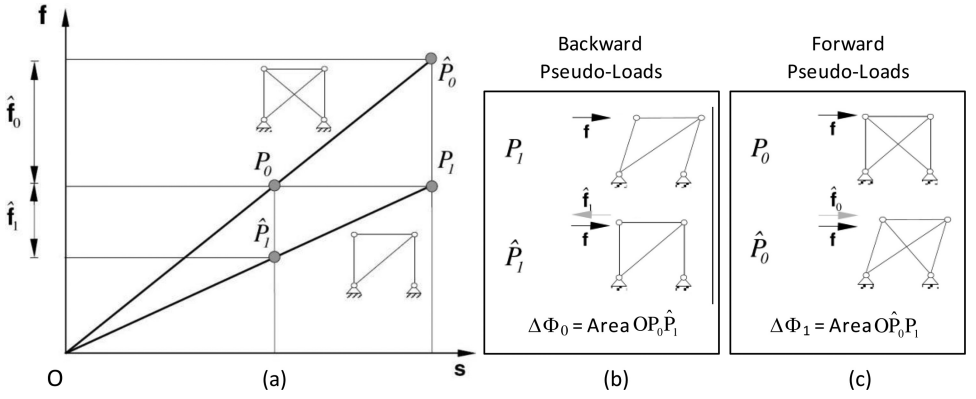

Figure 6.2 Force $\mathbf{f} = \mathbf{f}_0 = \mathbf{f}_1$ versus displacement $\mathbf{s}$ of a truss system in the intact state and after elimination of one member (adapted from Biondini & Restelli 2008). (a) Force-displacement diagrams. (b) Backward pseudo-loads (effects of repair). (c) Forward pseudo-loads (effects of damage).

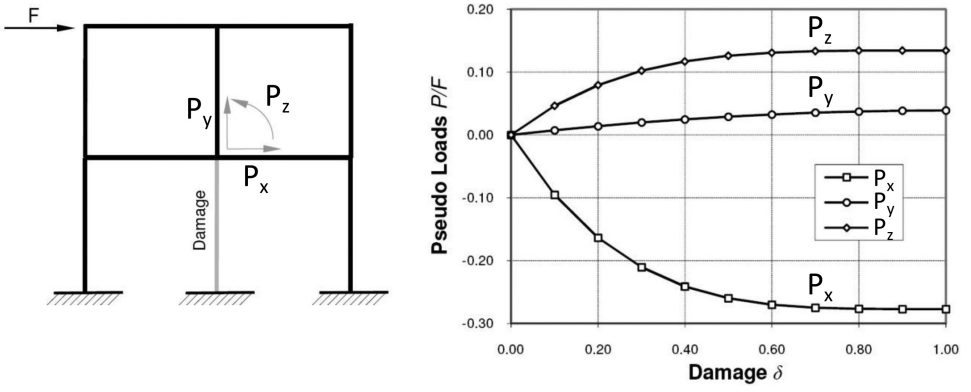

Figure 6.3 Backward pseudo-loads for a frame system undergoing damage of one column (adapted from Biondini & Restelli 2008).

In a dual way, the displacement vector of the damaged system $\mathbf{s}_1$ can be related to the displacement vector of the intact system $\mathbf{s}_0$ as follows:

$$\mathbf{s}_1 = \mathbf{s}_0 + \mathbf{K}_0^{-1}\hat{\mathbf{f}}_0 = \mathbf{K}_0^{-1}(\mathbf{f}_0 + \hat{\mathbf{f}}_0) \tag{6.18}$$

$$\hat{\mathbf{f}}_0 = -(\mathbf{K}_1 - \mathbf{K}_0)\mathbf{s}_1 + (\mathbf{f}_1 - \mathbf{f}_0) = -\Delta\mathbf{K}\mathbf{s}_1 + \Delta\mathbf{f} \tag{6.19}$$

where $\hat{\mathbf{f}}_0$ is a vector of nodal forces equivalent to the effects of damage (Figure 6.2c). This vector represents the additional nodal forces that must be applied to the intact system to achieve the nodal displacements of the damaged system, and it is called *forward*

pseudo-load vector (Biondini & Restelli 2008). Backward and forward pseudo-loads can be related as follows:

$$\mathbf{K}_0^{-1}\hat{\mathbf{f}}_0 + \mathbf{K}_1^{-1}\hat{\mathbf{f}}_1 = 0 \tag{6.20}$$

The concept of pseudo-loads can be usefully exploited to define two energy-based indicators related to the structural performance of both the intact system and the damaged system (Biondini & Restelli 2008). The first one of these indicators is the difference of stored energy Φ between the intact system (Φ_0) and the damaged system after the application of the backward pseudo-loads ($\hat{\Phi}_1$):

$$\Delta\Phi_0 = \Phi_0 - \hat{\Phi}_1 = \frac{1}{2}\mathbf{s}_0^T\mathbf{f}_0 - \frac{1}{2}\mathbf{s}_0^T(\mathbf{f}_1 + \hat{\mathbf{f}}_1) = -\frac{1}{2}\mathbf{s}_0^T(\hat{\mathbf{f}}_1 + \Delta\mathbf{f}) \tag{6.21}$$

The area $OP_0\hat{P}_1$ in Figure 6.2a represents the energy $\Delta\Phi_0$ for the case $\Delta\mathbf{f} = \mathbf{0}$. The second indicator is the difference of stored energy Φ between the intact system after the application of the forward pseudo-loads ($\hat{\Phi}_0$) and the damaged system (Φ_1):

$$\Delta\Phi_1 = \hat{\Phi}_0 - \Phi_1 = \frac{1}{2}\mathbf{s}_1^T(\mathbf{f}_0 + \hat{\mathbf{f}}_0) - \frac{1}{2}\mathbf{s}_1^T\mathbf{f}_1 = \frac{1}{2}\mathbf{s}_1^T(\hat{\mathbf{f}}_0 - \Delta\mathbf{f}) \tag{6.22}$$

The area $O\hat{P}_0P_1$ in Figure 6.2a represents the energy $\Delta\Phi_1$ for the case $\Delta\mathbf{f} = \mathbf{0}$.

6.3.3 *Failure Loads and Failure Times*

A failure of a system is generally associated to the violation of one or several limit states. Limit states of interest at ultimate conditions are the occurrence of the first local failure of a critical cross-section, that represents a warning for initiation of damage propagation, and the global collapse of the structural system. Denoting $\lambda \geq 0$ a scalar multiplier of the live loads, these limit states can be identified by the limit load multipliers λ_1 and λ_c associated to the reaching of first local failure and the structural collapse, respectively. Since the structural performance deteriorates over time, the functions $\lambda_1 = \lambda_1(t)$ and $\lambda_c = \lambda_c(t)$ need to be evaluated by means of time-variant structural analyses taking into account the effects of the damage process. In particular, the limit multipliers λ_1 and λ_c can effectively be computed at each time instant under the hypotheses of linear elastic behavior up to first local failure, and perfect plasticity at structural collapse, respectively (Biondini & Frangopol 2008, 2010a, Biondini 2009).

For structural systems the identification of the local failure modes and of their occurrence in time can represent crucial information to maintain a suitable level of performance and to avoid collapse over the structural lifetime (Biondini & Frangopol 2010b, Biondini 2012). In fact, repairable local failures can be considered as a warning of possible occurrence of more severe and/or not repairable failures. Failure times should be computed to this purpose and the time interval between the first local failure and structural collapse, or the elapsed time between these two types of failures, could represent an effective indicator of the damage tolerance of the system and its ability to be repaired after local failures.

The structural lifetimes T_1 and T_c associated to the occurrence of the first local failure and the structural collapse, respectively, can be evaluated as follows:

$$T_1 = \min\{t|\lambda_1(t) < 1\} \tag{6.23}$$

$$T_c = \min\{t|\lambda_c(t) < 1\} \tag{6.24}$$

The elapsed time between failures ΔT is the time interval between the first local failure and structural collapse, or:

$$\Delta T = T_c - T_1 \tag{6.25}$$

This concept can be extended to investigate all sequential local failure modes up to collapse and their activation in time (Biondini 2012).

6.4 Measure of Structural Robustness

Structural robustness can be viewed as the ability of a system to suffer an amount of damage not disproportionate with respect to the causes of the damage itself (Ellingwood & Dusenberry 2005). According to this general definition, a measure of structural robustness should arise by comparing the structural performance of the system in the original state, in which the structure is fully intact, and in a perturbed state, in which a prescribed damage scenario is applied (Frangopol & Curley 1987, Biondini & Restelli 2008, Biondini et al. 2008). To this aim, the variation of structural performance has to be compared with the corresponding amount of damage to provide meaningful information for robustness evaluations.

Based on this approach, the performance indicators are used as state variables, and a direct measure of structural robustness can be obtained through time-variant robustness indices $\rho = \rho(t)$ that are dimensionless functions of these variables varying in the range $[0, 1]$, with $\rho = 1$ for the undamaged system at the initial time $t = 0$. It is worth noting that the quantification of these indices is in general not sufficient to quantify structural robustness. The index ρ has to be related with the amount of damage to provide a measure of robustness in terms of a functional $\rho = \rho(\delta)$ or $\rho = \rho(\Delta)$.

The following time-variant measure has been proposed in Biondini (2009) to quantify structural robustness:

$$R(\rho, \Delta) = \rho(t)^{\alpha} + \Delta(t)^{\alpha} \tag{6.26}$$

where $R = R(\rho, \Delta)$ is a robustness factor, and α is a shape parameter of the boundary $R = R(\rho, \Delta) = 1$. The structural system is robust when the criterion is satisfied ($R \geq 1$), and not robust otherwise ($R < 1$). This concept is illustrated in Figure 6.4a.

As shown in Figure 6.4b, the value of the parameter α can be selected according to the acceptable level of damage susceptibility. A value $\alpha = 1$, which indicates a proportionality between acceptable loss of performance and damage, should be appropriate in most cases. Values $\alpha > 1$ could be required for structures of strategic importance, and values $\alpha < 1$ should be avoided, since they allow for disproportionate damage effects, or used for temporary structures.

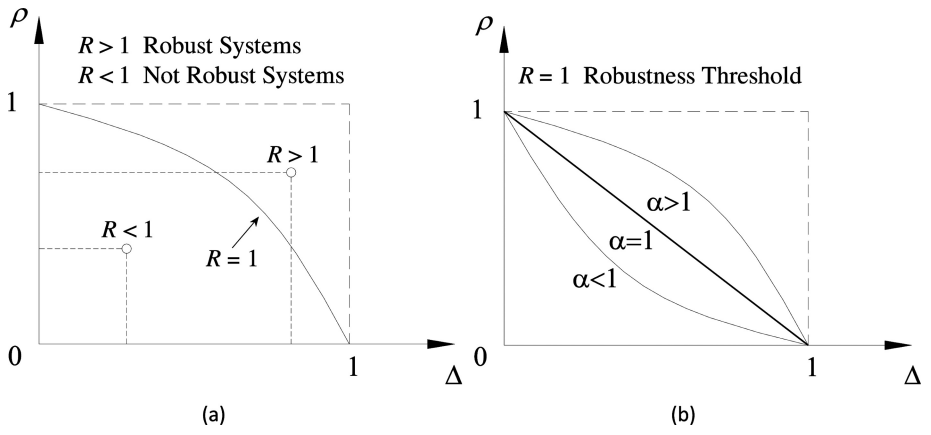

Figure 6.4 Performance index ρ versus damage index Δ (adapted from Biondini & Frangopol 2012). (a) Robustness factor $R = R(\rho, \Delta)$. (b) Role of the parameter α on the robustness threshold $R = 1$.

The relationship $R = R(\rho, \Delta)$ is time-variant and nonlinear. For this reason, it is recommended that the robustness criterion $R(t) \geq 1$ is verified at discrete points in time over the whole structural lifetime. In particular, integral measures of robustness based on the following formulation:

$$R' = \int_0^1 \rho(\Delta) d\Delta \tag{6.27}$$

should be avoided since they can provide only average indications over the lifetime and are not able to describe the actual level of structural robustness (Starossek & Haberland 2011).

6.5 Role of Performance Indicators and Structural Integrity

6.5.1 *A Comparative Study*

To discuss the effectiveness of the proposed performance indicators, the structural robustness of the truss system shown in Figure 6.5 is investigated under the progressive damage of each one of its members (m = lumped nodal mass). The cross-section of all members is circular, and for the damaged member an external layer of uniform thickness is removed, as shown in Figure 6.1 for cross-section ①.

The following robustness indices under linear elastic behavior are considered:

$$\rho_d = \frac{d_1}{d_0} \tag{6.28}$$

$$\rho_\tau = \frac{\tau_1}{\tau_0} \tag{6.29}$$

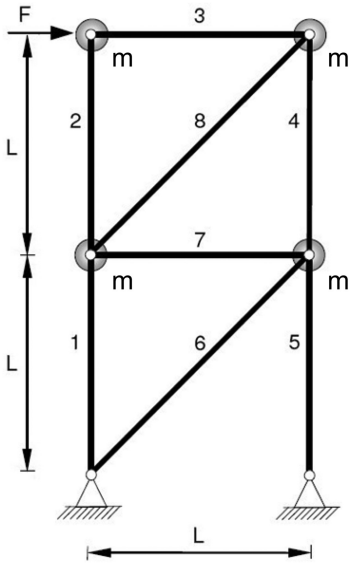

Figure 6.5 Truss system undergoing damage of one member (adapted from Biondini & Restelli 2008).

$$\rho_c = \frac{c_0}{c_1} \tag{6.30}$$

$$\rho_T = \frac{T_{n0}}{T_{n1}} \tag{6.31}$$

$$\rho_s = \frac{s_0}{s_1} \tag{6.32}$$

$$\rho_\Phi = \frac{\Phi_0}{\Phi_1} \tag{6.33}$$

$$\rho_0 = 1 - \frac{\Delta\Phi_0}{\Phi_0} \tag{6.34}$$

$$\rho_1 = 1 - \frac{\Delta\Phi_1}{\hat{\Phi}_0} \tag{6.35}$$

In general, structural performance should decrease due to damage, leading to $\rho(\delta') \leq \rho(\delta'')\ \forall\, \delta' > \delta''$. However, it should be noted that performance indicators could also increase with damage. This may happen for example when damage involves material hardening.

The results are presented in Figure 6.6 where it can be noted that, globally, the robustness indices $\rho = \rho(\delta)$ allow the evaluation of the role played by each member

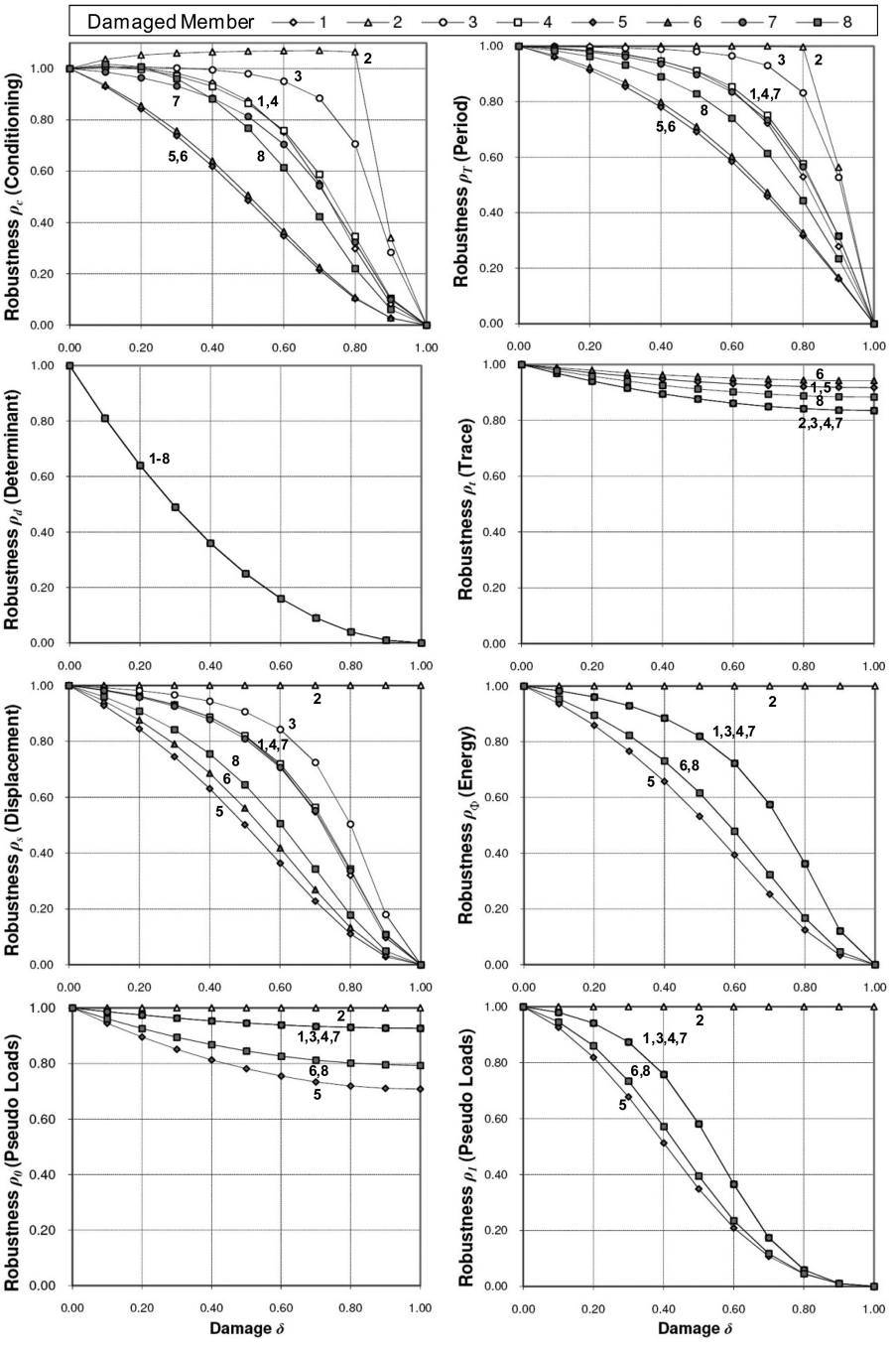

Figure 6.6 Truss system undergoing damage of one member. Robustness indices ρ versus damage index δ (adapted from Biondini & Restelli 2008).

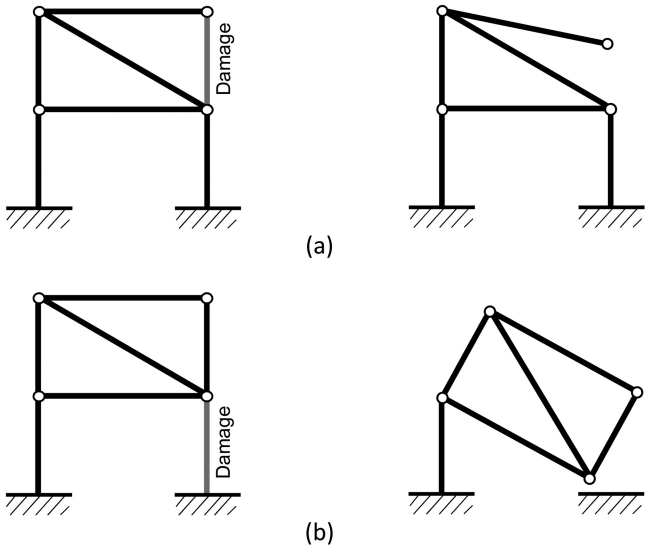

Figure 6.7 Types of structural failure. (a) Local failure. (b) Global failure.

on the overall performance of the damaged system. However, the following critical aspects are outlined:

- The index ρ_c may increase under damage evolution, with values $\rho_c > 1$. This is not consistent with the trend observed for the other indices.
- The index ρ_d is not able to catch the different role played by each member, since it has the same value regardless of the member that is undergoing damage.
- The indices ρ_τ and ρ_0 show a very little sensitivity to damage and are not able to identify the failure condition $\rho = 0$ associated with $\delta = 1$.

Therefore, the indices ρ_c, ρ_d, ρ_τ, and ρ_0, are not suitable to effectively describe the effects of damage on the structural performance. In contrast, the indices ρ_T, ρ_s, ρ_Φ, and ρ_1, can effectively be used to measure the structural robustness.

6.5.2 *Structural Integrity Index*

A robustness index should be able to identify the structural collapse by assuming at failure the value $\rho = 0$. However, in robustness evaluations it may also be crucial to quantify the severity of a structural failure with regards to its consequences. For example, the global collapse of a whole structural system should be considered much more important than the local collapse of a single member or a portion of the structure (Figure 6.7). An importance measure of structural failure could be provided by the following structural integrity index (Biondini & Restelli 2008):

$$\rho_V = \frac{V_1}{V_0} \tag{6.36}$$

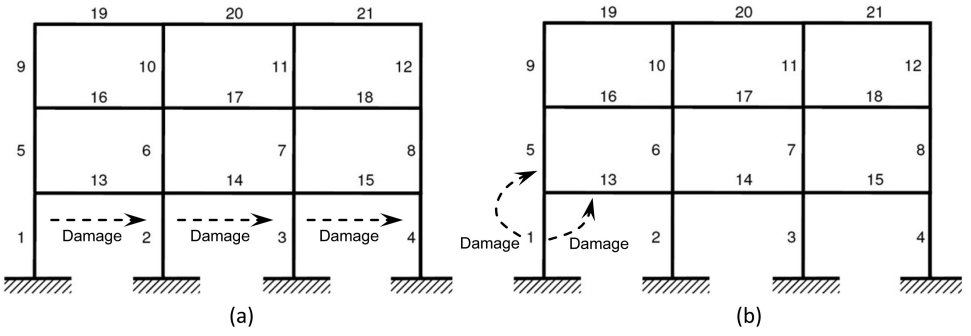

Figure 6.8 Mechanisms of damage propagation (adapted from Biondini & Restelli 2008). (a) Directionality-based mechanism. (b) Adjacency-based mechanism.

where V_1 is the portion of structural volume V_0 which remains intact after damage. Failed members involved in a collapse mechanism can be identified based on the eigenvectors $\mathbf{s}_i$ of the stiffness matrix $\mathbf{K}$ associated with the eigenvalues $\vartheta_i(\mathbf{K}) = 0$.

The values of the structural integrity index $\rho_{V,k}$ associated to the failure of each member k of the truss structure shown in Figure 6.5 are $\rho_{V,2} = \rho_{V,3} = 0.75$, $\rho_{V,4} = \rho_{V,8} = 0.50$, $\rho_{V,1} = \rho_{V,7} = 0.25$, and $\rho_{V,5} = \rho_{V,6} = 0$. It is worth noting that also members not directly exposed to damage may fail. For example, a complete damage of member 8 causes also the failure of members 2, 3, and 4.

6.6 Damage Propagation

6.6.1 *Propagation Mechanisms*

For redundant structures, local damage or failure of a member usually does not involve the collapse of the whole system. As a consequence, after failure of one member other members may fail, and the sequence of local failures propagates throughout the overall system until its collapse is reached. The mechanism of damage propagation is usually related to the causes of the damage itself. Two alternative propagation mechanisms, defined as directionality-based and adjacency-based, are investigated (Biondini & Restelli 2008).

In the directionality-based mechanism, damage propagates along the direction normal to the axis of the first failed member. For example, with reference to the frame system shown in Figure 6.8a, the damage of member 1 is followed in sequence by the damage of members 2, 3, and 4. The directionality-based mechanism is typical of damage induced by severe loadings, such as explosions or impacts, which generally tends to propagate along the direction of loading.

In the adjacency-based mechanism, damage propagates towards the members directly connected with other members already damaged. For example, with reference to the frame system shown in Figure 6.8b, the damage of member 1 can be followed by the damage of the members 5 and 13. The adjacency-based mechanism is typical of damage induced by aggressive agents, like chlorides, which generally tends to propagate through the structure based on diffusion processes.

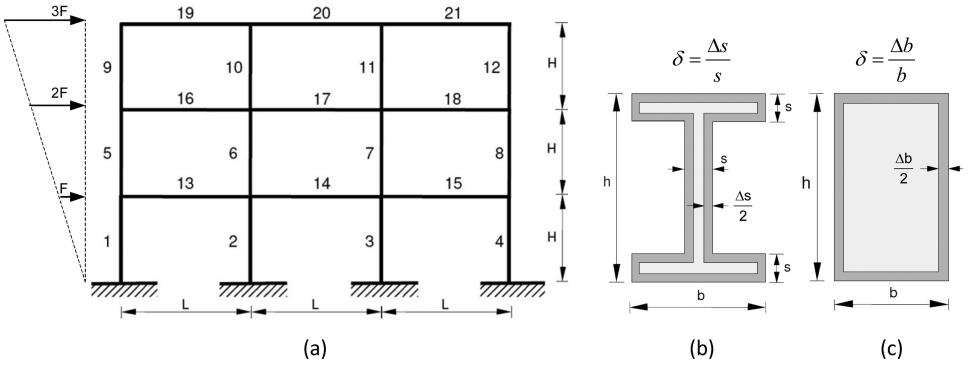

Figure 6.9 Frame system under damage (adapted from Biondini & Restelli 2008). (a) Geometry ($L/H = 2$), structural scheme, and loading. Cross-sections of (b) beams ($h/s = 15$) and (c) columns ($h/b = 1.5$).

6.6.2 *Fault-Tree Analysis*

Starting from the local definition of damage, and based on a prescribed propagation mechanism, a damage scenario at the system level can be developed by using a damage-sensitive fault-tree analysis (Biondini & Restelli 2008). In such a way, all the feasible damage paths associated with the propagation mechanism and the actual topology of the system can be described by branched networks where the level of activation of each nodal connection is properly tuned to account for the prescribed amount of local structural damage.

To describe the main features of this approach, the structural robustness of the frame system shown in Figure 6.9a is evaluated under a distribution of lateral loads. The cross-sections of beams and columns, as well as the assumed cross-sectional damage patterns, are shown in Figures 6.9b and 6.9c. Elastic behavior is assumed. A three-level fault-tree analysis is carried out by assuming an adjacency-based propagation mechanism and a total damage ($\delta = 1$) for each member. The results are represented in Figure 6.10 in terms of contoured branched network for the displacement-based robustness index ρ_s defined in Equation (6.32). This mapping provides a comprehensive description and a quantitative measure of the structural resources of the system with respect to all the considered damage propagation paths.

6.7 Structural Robustness and Progressive Collapse

Local damage or failure of a member usually involves a redistribution of internal forces among the other members of the structural system. As a consequence, if the amount of redistributed forces is large enough, other members may fail and the sequence of local failures may propagate throughout the overall system until its collapse is reached. A possible way to avoid this type of progressive collapse is to design robust structures for which alternate load paths are possible and the most critical members are properly protected from accidental- or environmental-induced damage.

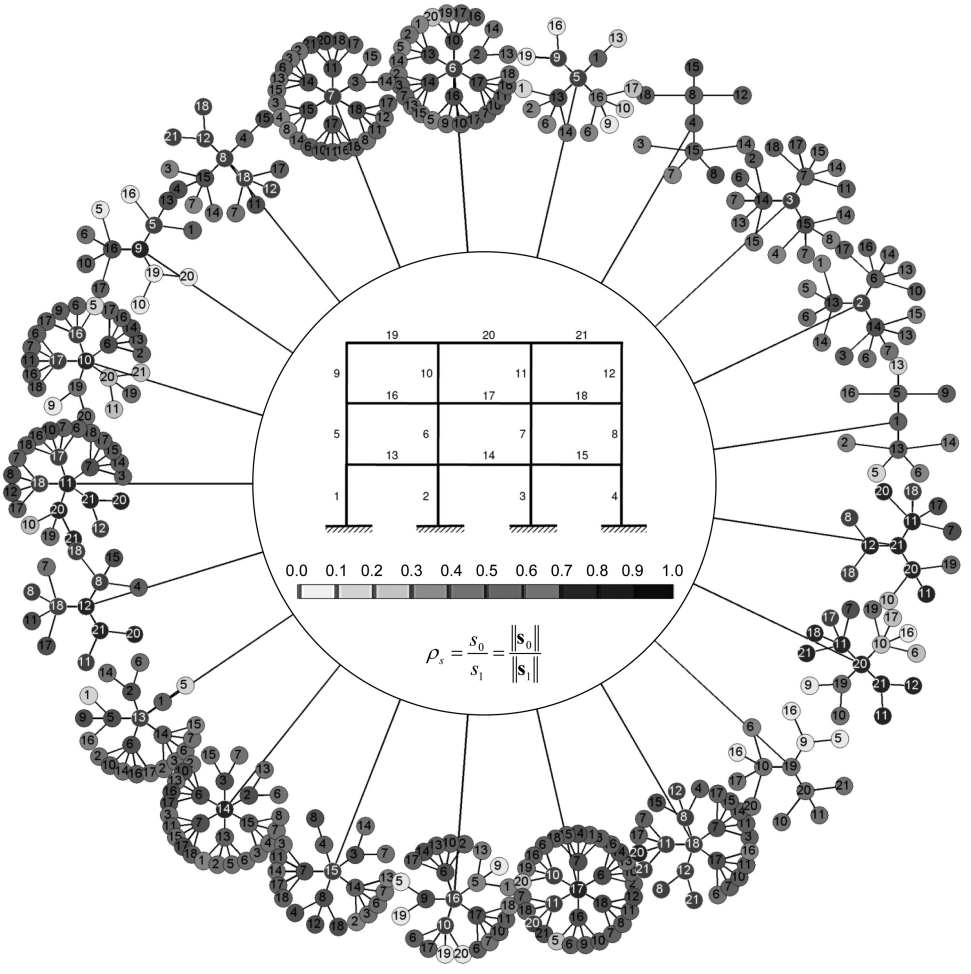

Figure 6.10 Three-level fault-tree robustness analysis of a frame system undergoing total damage ($\delta = 1$) of each member with adjacency-based propagation mechanism (adapted from Biondini & Restelli 2008): contoured branched network of structural robustness (displacement-based robustness index ρ_s).

To highlight the role of robustness on progressive collapse, a preliminary investigation is developed with reference to the simple parallel systems composed of $n = 6$ truss members shown in Figure 6.11 (Biondini et al. 2008). The force F_k carried by each member $k = 1, 2, \ldots, 6$, is a portion ν_k of the total applied load F in such a way that the equilibrium is satisfied:

$$\nu_k = \frac{F_k}{F}, \quad \sum_1^n \nu_k = 1 \tag{6.37}$$

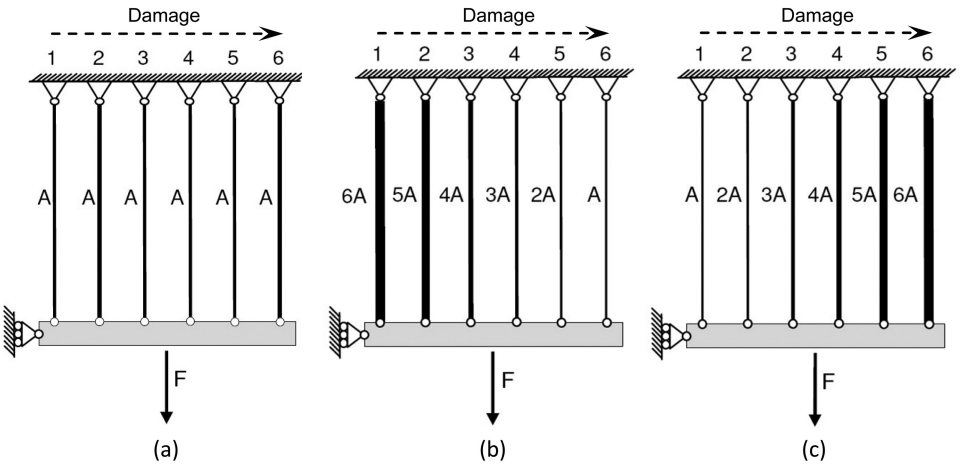

Figure 6.11 Parallel systems undergoing damage of all members (adapted from Biondini et al. 2008). (a) All bars $k = 1,\ldots,6$ have the same initial area $A_k = A$. (b) The k-th bar has initial area $A_k = (n-k+1)A$ (damage proceeds from the strongest member to the weakest one). (c) The k-th bar has initial area $A_k = kA$ (damage proceeds from the weakest member to the strongest one).

Due to the static indeterminacy of the problem, the coefficients ν_k depend on the geometrical and mechanical properties of the members, as well as on the damage state of the system.

All members are assumed to have circular cross-section with uniform damage along the external boundary, as shown in Figure 6.1 for cross-section 1. For each member k the deterioration of the cross-sectional area is described by the corresponding damage index $\delta_k \in [0; 1]$. Damage is assumed to develop in each member and proceed from a member k to the adjacent one $(k+1)$ in a progressive and continuous way. Based on this assumption, the damaged state of the system can be described by a total cumulative damage function $\Delta_k \in [0; n]$ defined as follows:

$$\Delta_k = \sum_{i=1}^{k} \delta_i = (k-1) + \delta_k \tag{6.38}$$

Three cases are studied: (a) all bars k have the same initial area $A_k = A$ (Figure 6.11a); (b) each bar k has initial area $A_k = (n-k+1)A$, in such a way that damage proceeds from the strongest member to the weakest one (Figure 6.11b); (c) each bar k has initial area $A_k = kA$, in such a way that damage proceeds from the weakest member to the strongest one (Figure 6.11c). For all cases the material behavior is described by a bilinear constitutive law with hardening. By denoting f_y and ε_y the stress and strain values at yielding, and f_u and ε_u the stress and strain values at ultimate, an overstrength ratio $f_u/f_y \cong 1.5$ and a ductility ratio $\varepsilon_u/\varepsilon_y \cong 10$ are assumed.

The displacement-based index ρ_s defined in Equation (6.32) is considered. As damage increases, the robustness ρ of the system changes and a redistribution of the internal

forces v_k occurs. The evolution of this process depends on the ratio η between the applied load F and the load $F_y = f_y \Sigma_k A_k$ associated with the first yielding of the system:

$$\eta = \frac{F}{F_y} \tag{6.39}$$

Structural collapse is reached when the propagation of damage leads to failure of all members. In this limit condition the robustness index vanishes and total damage is identified by the following threshold:

$$\Delta_{k,c} = \min\{\Delta_k | \rho(\Delta_k) = 0\} \tag{6.40}$$

Therefore, the functions $\rho = \rho(\Delta_k)$ and $v = v(\Delta_k)$ with $\Delta_k \leq \Delta_{k,c}$ define the paths followed by the system towards its progressive collapse. Figure 6.12 shows the robustness index ρ and the internal forces v_k as a function of the cumulative damage Δ_k for different levels of the load ratio η and for each one of the three cases studied. These results can be used to check if a progressive collapse occurs under prescribed loading and damaging scenarios or, conversely, to evaluate the limit load and/or the damage threshold associated with the occurrence of progressive collapse.

It should be noted that the values associated with case (a) are in between the results associated with cases (b) and (c). For case (b) damage starts in the strongest members, which progressively exchange their leading role with the weakest members. Consequently, this case is characterized by the lower robustness and it is more prone to reach a progressive collapse. On the contrary, for case (c) damage starts in the weakest members and the leading role of the strongest members can be fully exploited until collapse.

However, the two structures associated with cases (b) and (c) will have the same expected performance if the direction of damage propagation is not defined. For this reason, the configuration in case (a) should be considered as the best one for a robust design, unless there are reasons for considering one direction of damage propagation more probable than others. More generally, it can be concluded that very strong members playing a disproportionate role in the structural system should be avoided in design of robust structures. Nevertheless, when this is not possible adequate remedy should be adopted to properly protect the most important members against occurrence of damage.

6.8 Structural Robustness and Static Indeterminacy

The role of static indeterminacy in the design of robust structures is investigated. To this aim, the $n = 6$ parallel systems shown in Figure 6.13 are firstly considered (Biondini et al. 2008). For each k-bar system, with $k = 1, 2, \ldots, 6$, the degree of static indeterminacy is $I = (k - 1)$. All members are identical and their cross-sectional shape and material behavior are the same as in the previous example. Damage is assumed to develop in one member only and it is quantified by the corresponding damage index $\delta \in [0; 1]$.

Figure 6.14 presents the evolution of the displacement-based robustness index ρ_s defined in Equation (6.32) as a function of the damage index δ (Figure 6.14a) and

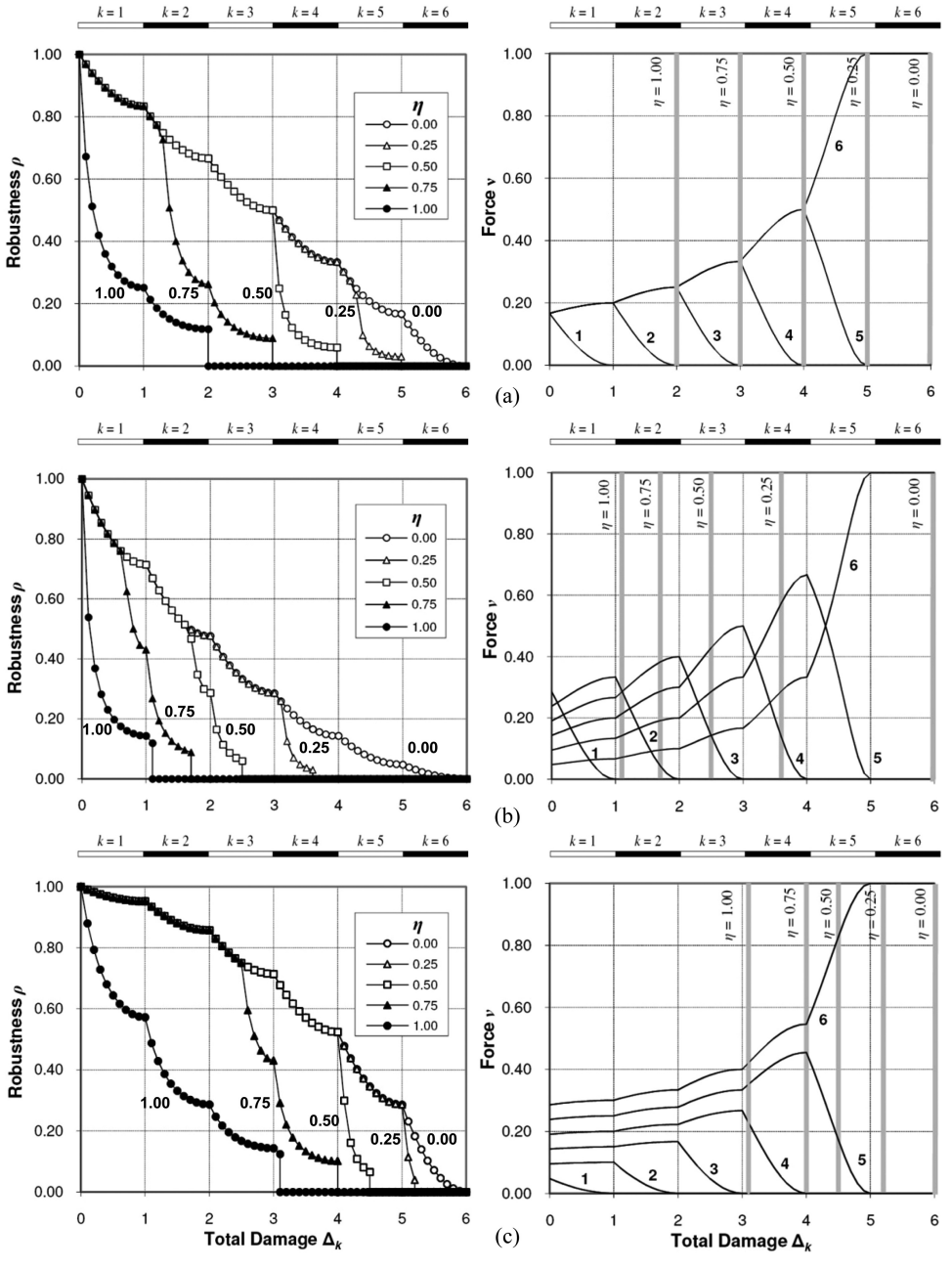

Figure 6.12 Parallel systems undergoing damage of their members: displacement-based robustness index ρ_s and internal forces ν_k versus the cumulative damage Δ_k for different levels of the load ratio η (adapted from Biondini et al. 2008). (a) $A_k = A$. (b) $A_k = (n - k + 1)A$ (damage proceeds from the strongest member to the weakest one). (c) $A_k = kA$ (damage proceeds from the weakest member to the strongest one).

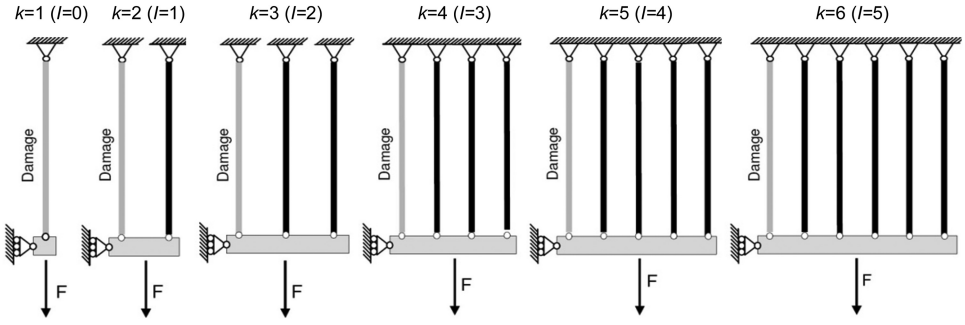

Figure 6.13 Parallel systems undergoing damage of one member (adapted from Biondini et al. 2008).

of the degree of static indeterminacy I (Figure 6.14b), for different values of the load ratio η. These results show that robustness increases as static indeterminacy increases. However, it is worth noting that only a certain degree of static indeterminacy (i.e., $I \leq 2$) provides a significant contribution to structural robustness for all load ratios, and the importance of this contribution increases with the amount of damage.

For higher levels of static indeterminacy (i.e. $I \geq 3$), the beneficial effects are in general less important, and the contribution to structural robustness tends to be significant only for severe damage and very high values of the load ratio η. Clearly, higher levels of static indeterminacy would be required when more than one member is affected by damage. In general, it can be concluded that in design of robust structures the degree of static indeterminacy should be adequately allocated as a function of the expected amount of damage.

In the previous example, robustness increases as static indeterminacy increases. However, this result cannot be generalized, since an increase in the degree of static indeterminacy does not necessarily lead to an increase of robustness. Consider for example the $n = 4$ mixed series-parallel truss systems shown in Figure 6.15 (Biondini et al. 2008). The degree of static indeterminacy of each system $k = 1, 2, \ldots, 4$, is $I = 2 \times (k - 1)$. All members are identical with hollowed circular cross-section and uniform damage along the external boundary, as shown in Figure 6.1 for cross-section 2. The material behavior is the same as in the previous examples. Damage is assumed to simultaneously develop in the two adjacent members located at the bottom of the truss beam at the middle span, and its evolution is described by the corresponding damage index $0 \leq \delta \leq 1$.

Figure 6.16 depicts the evolution of the robustness index ρ as a function of the damage index δ (Figure 6.16a) and of the degree of static indeterminacy I (Figure 6.16b), for different values of the load ratio η. These results confirm that only a certain degree of static indeterminacy (i.e. $I \leq 2$) provides a significant contribution to structural robustness for all load ratios, particularly when severe damage tends to develop.

For higher levels of static indeterminacy (i.e. $I \geq 4$), the beneficial effects are reduced and structural robustness tends to decrease as the degree of static indeterminacy increases. Clearly, different trends may arise when different damage scenarios are considered. However, this statement can be generalized by concluding that in design

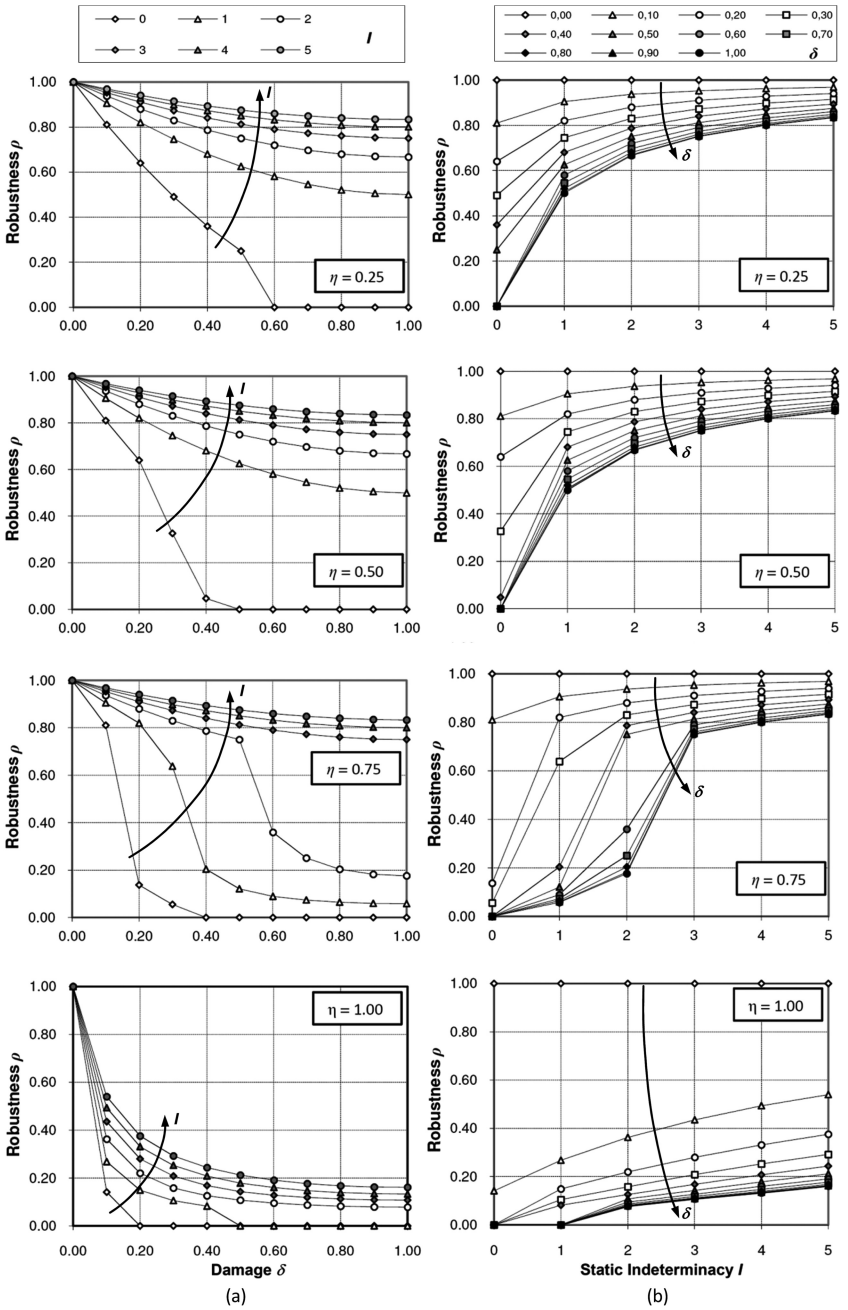

Figure 6.14 Parallel systems undergoing damage of one member: displacement-based robustness index ρ_s versus (a) damage δ and (b) degree of static indeterminacy I, for different values of load ratio η (adapted from Biondini et al. 2008).

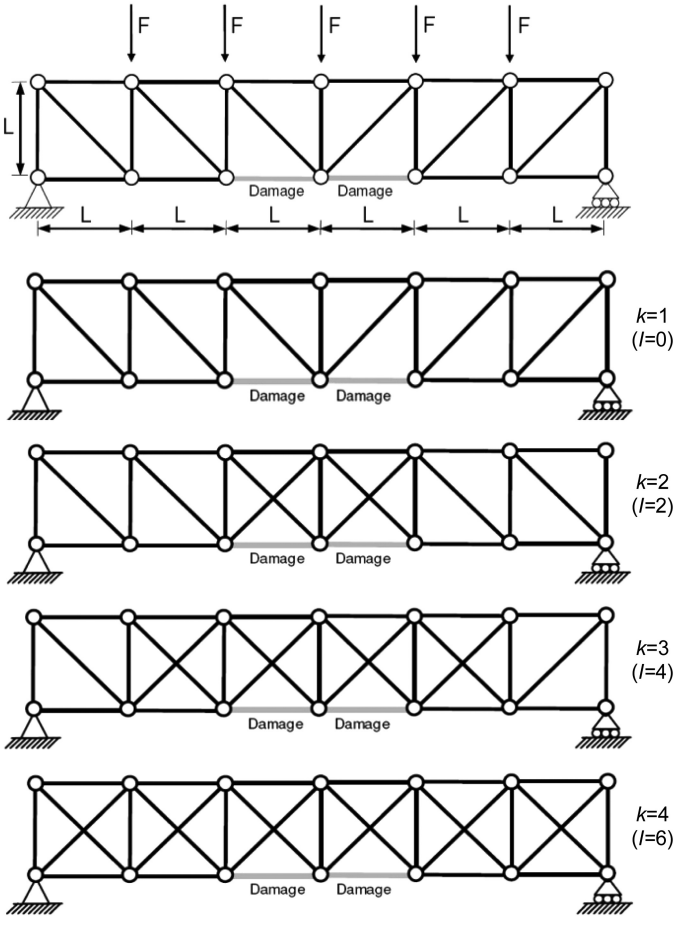

Figure 6.15 Truss systems undergoing damage of two members (adapted from Biondini et al. 2008).

of robust structures an adequate degree of static indeterminacy should be provided according not only with the amount, but also with the expected location of structural damage.

6.9 Structural Robustness, Structural Redundancy and Failure Times

The terms robustness and redundancy, even though they are often used as synonymous, denote different properties of the structural system (Biondini et al. 2010a, 2013). Structural redundancy is the ability of the system to redistribute among its members the load which can no longer be sustained by some other damaged members after the occurrence of a local failure (Frangopol & Curley 1987, Frangopol & Klisinski 1989, Frangopol et al. 1992, Biondini et al. 2008, Biondini & Frangopol 2010a).

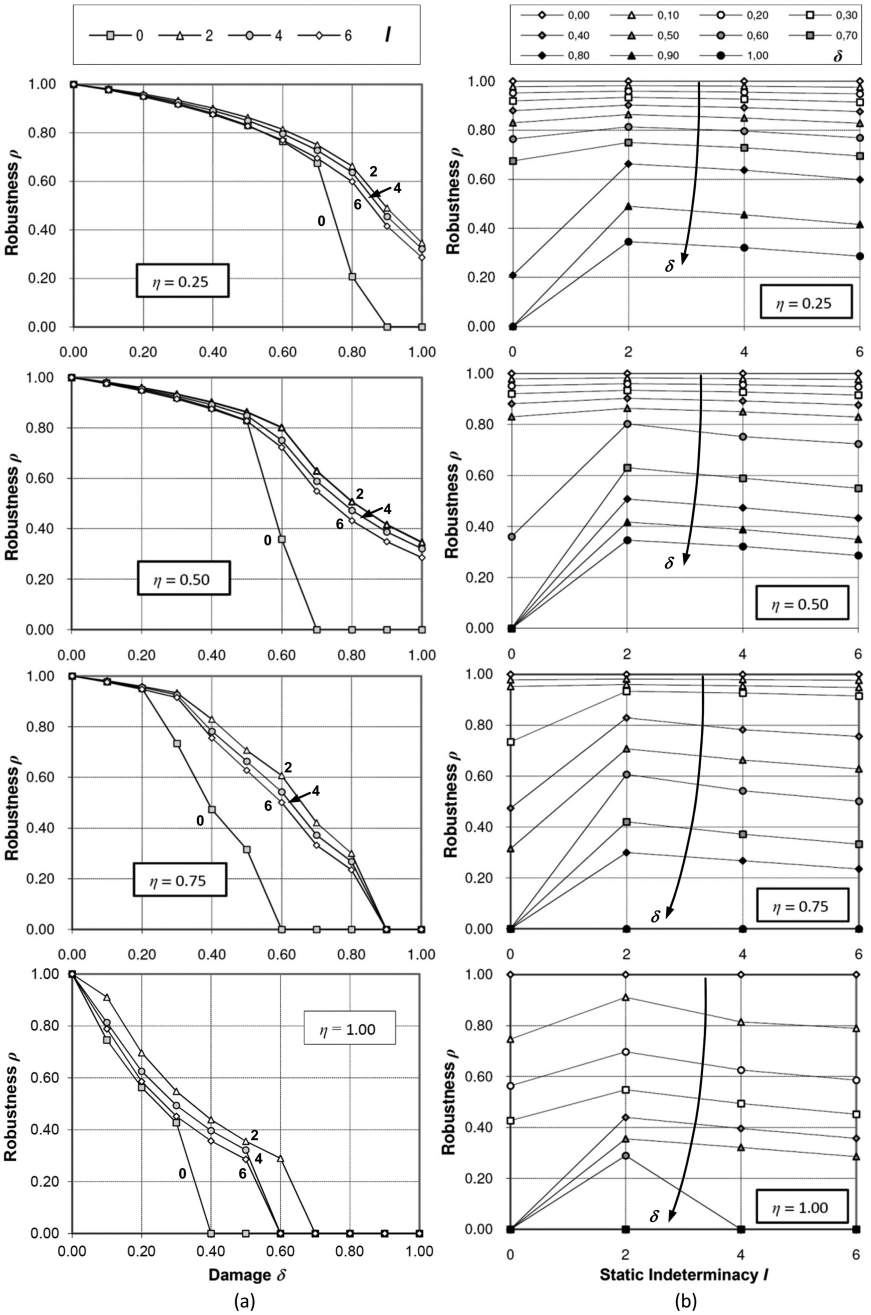

Figure 6.16 Truss systems undergoing damage of two members: displacement-based robustness index ρ_s versus (a) damage δ and (b) degree of static indeterminacy l, for different values of load ratio η (adapted from Biondini et al. 2008).

Redundancy is usually associated with the degree of static indeterminacy. However, it has been demonstrated that the degree of static indeterminacy is not a consistent measure for structural redundancy. In fact, structures with lower degrees of static indeterminacy can have a greater redundancy than structures with higher degrees of static indeterminacy (Frangopol & Curley 1987). Moreover, structural redundancy refers to a prescribed point in time and does not provide a measure of the failure rate, which depends on the damage scenario and damage propagation mechanism. Failure times and the elapsed time between local failures and structural collapse should be computed to this purpose (Biondini & Frangopol 2010b, 2013).

6.9.1 *Case Study*

The lifetime structural performance of the RC frame shown in Figure 6.17 is investigated in terms of robustness, redundancy, and failure times (Biondini & Frangopol 2013). The frame is subjected to a dead load $q = 32$ kN/m applied on the beam and a live load λF acting at top of the columns, with $F = 100$ kN.

The nonlinear constitutive laws of the materials are described in terms of stress-strain diagrams. For concrete, a Saenz's law in compression and an elastic-plastic model in tension are assumed, with the following nominal parameters: compression strength $f_c = -40$ MPa; tension strength $f_{ct} = 0.25|f_c|^{2/3}$; initial modulus $E_{c0} = 9500|f_c|^{1/3}$; peak strain in compression $\varepsilon_{c0} = -0.20\%$; strain limit in compression $\varepsilon_{cu} = -0.35\%$; strain limit in tension $\varepsilon_{ctu} = 2f_{ct}/E_{c0}$. For steel, an elastic perfectly plastic model in both tension and compression is assumed, with yielding strength $f_{sy} = 500$ MPa and elastic modulus $E_s = 210$ GPa.

The frame system is designed to have cross-sectional stiffness and bending strength capacities much larger in the beam than in the columns. Moreover, shear failures are avoided by a proper capacity design. In this way, a shear-type behavior can be assumed for the frame system, with the critical regions where plastic hinges are expected to occur located at the ends of the columns.

The structure is subjected to a diffusive attack from an aggressive agent located on the external surfaces of the columns with prescribed concentration C_0. The two exposure scenarios shown in Figure 6.17 are considered: (I) columns exposed on the outermost side only, and (II) columns exposed on the four sides. A nominal diffusivity coefficient $D = 10^{-11}$ m^2/sec is assumed. The Fick's equations which describe the diffusion process are solved numerically by means of cellular automata taking the stochastic effects in the mass transfer into account (Biondini et al. 2004). It is worth noting that for the case studied both deterministic and stochastic mass diffusion lead to comparable amount of damage over a lifetime $T = 50$ years (Biondini & Frangopol 2009). Figure 6.18 shows the deterministic maps of concentration $C(\mathbf{x}, t)/C_0$ for the two investigated exposure scenarios after 10, 20, 30, 40, and 50 years from the initial time of diffusion penetration.

6.9.2 *Corrosion Damage and Failure Loads*

The corrosion damage induced by diffusion is evaluated by assuming $C_s = C_0$, $\Delta t_s = 50$ years and $C_{cr} = 0$. This damage model reproduces a deterioration process with severe corrosion of steel, as may occur for carbonated or heavily chloride-contaminated concrete and high relative humidity, conditions under which the corrosion rate can reach

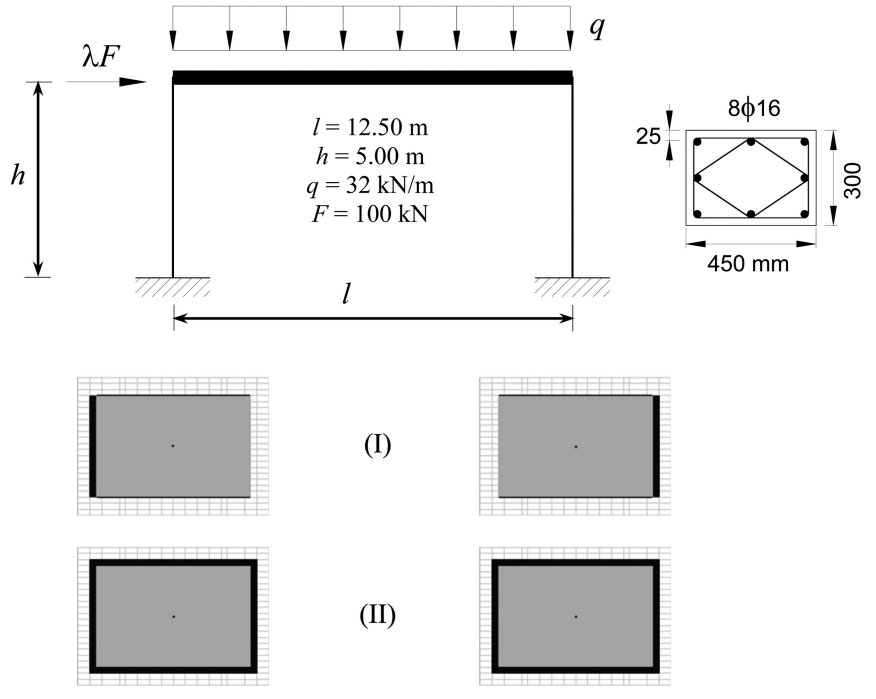

Figure 6.17 RC frame exposed to corrosion. Geometry, structural scheme, cross-section of the columns, loading condition and exposure scenarios (adapted from Biondini & Frangopol 2013). (I) Columns exposed on one side. (II) Columns exposed on four sides.

values above 100 μm/year (Bertolini et al. 2004). Figure 6.19 illustrates the evolution over a lifetime $T = 50$ years of the global damage index $\Delta = \Delta(t)$ representing the amount of corrosion steel damage over the structure for the two investigated exposure scenarios. The comparison of the results shows that, as expected, case (II) is the worst scenario in terms of global damage.

Figure 6.20 shows the corresponding evolution over time of the limit load multipliers $\lambda_1 = \lambda_1(t)$ and $\lambda_c = \lambda_c(t)$ associated to the reaching of first local yielding of steel reinforcement and structural collapse of the frame system, respectively. The comparison of the results shown in Figures 6.20a and 6.20b confirms that case (II) is the worst damage scenario also in terms of loss of load carrying capacities.

6.9.3 *Robustness and Redundancy*

Structural robustness is investigated under corrosion damage with respect to collapse. The ratio of the limit load multiplier $\lambda_c = \lambda_c(t)$ to its initial value $\lambda_{c0} = \lambda_c(0)$ is assumed as robustness index:

$$\rho(t) = \frac{\lambda_c(t)}{\lambda_{c0}} \tag{6.41}$$

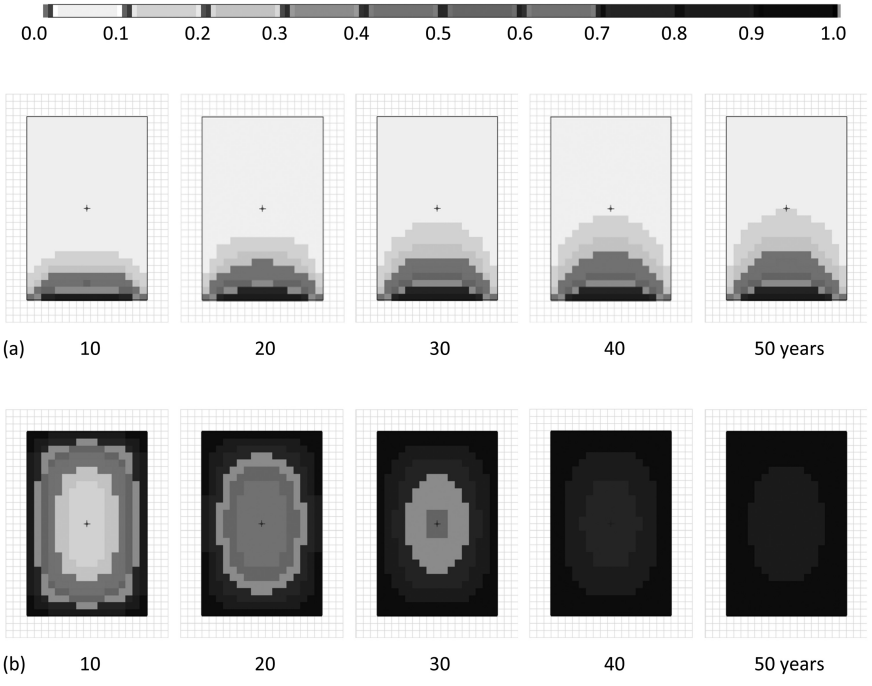

Figure 6.18 Maps of the concentration $C(\mathbf{x}, t)/C_0$ of the aggressive agent after 10, 20, 30, 40, and 50 years from the initial time of diffusion penetration (adapted from Biondini & Frangopol 2013). (a) Scenario (I) with exposure on one side. (b) Scenario (II) with exposure on four sides.

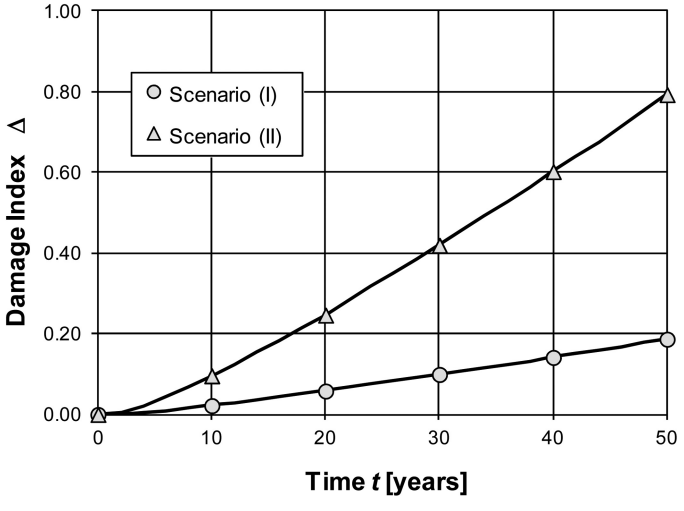

Figure 6.19 Time evolution of the global damage index Δ for scenario (I) with exposure on one side, and scenario (II) with exposure on four sides (adapted from Biondini & Frangopol 2013).

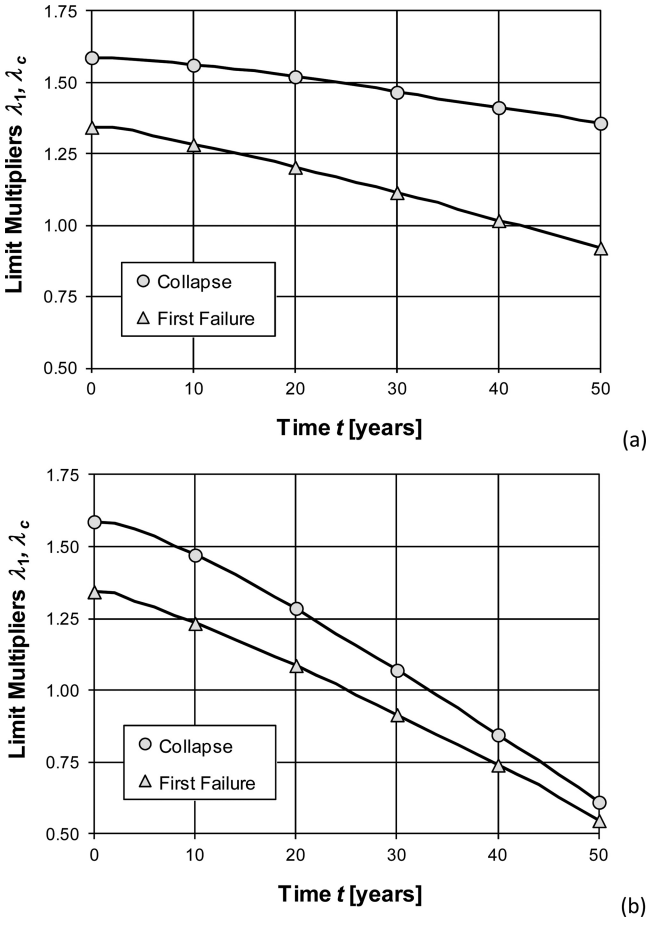

Figure 6.20 Time evolution of the limit load multipliers at first failure, λ_1, and structural collapse, λ_c (adapted from Biondini and Frangopol 2013). (a) Scenario (I) with exposure on one side. (b) Scenario (II) with exposure on four sides.

The robustness index $\rho = \rho(t)$ is compared with the global damage index $\Delta = \Delta(t)$ according to the robustness criterion $R(\rho, \Delta) = R(t) = 1$. Figure 6.21 shows the time evolution of the robustness factor $R = R(t)$ of the frame system computed with $\alpha = 1$ for the two investigated scenarios. These results highlight that the frame is robust over the lifetime, and that case (I) with localized corrosion is the worst damage scenario for structural robustness.

The ability of the system to redistribute the load after the first local failure up to collapse depends on the difference between the limit multipliers $\lambda_c = \lambda_c(t)$ and $\lambda_1 = \lambda_1(t)$.

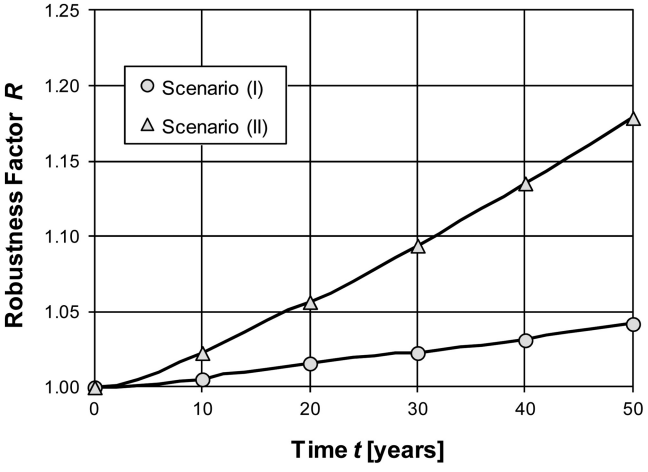

Figure 6.21 Time evolution of the robustness factor R with $\alpha = 1$ for scenario (I) with exposure on one side, and scenario (II) with exposure on four sides (adapted from Biondini & Frangopol 2013).

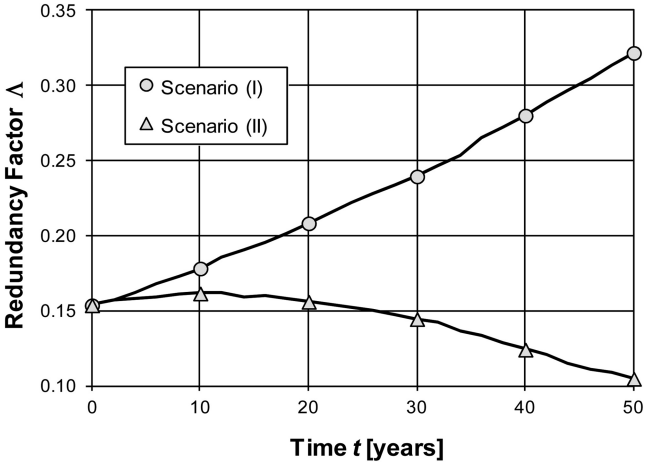

Figure 6.22 Time evolution of the redundancy factor Λ for scenario (I) with exposure on one side, and scenario (II) with exposure on four sides (adapted from Biondini & Frangopol 2013).

Therefore, the following quantity is assumed as time-variant measure of redundancy (Biondini & Frangopol 2010a):

$$\Lambda(\lambda_1, \lambda_c) = \frac{\lambda_c(t) - \lambda_1(t)}{\lambda_c(t)} \tag{6.42}$$

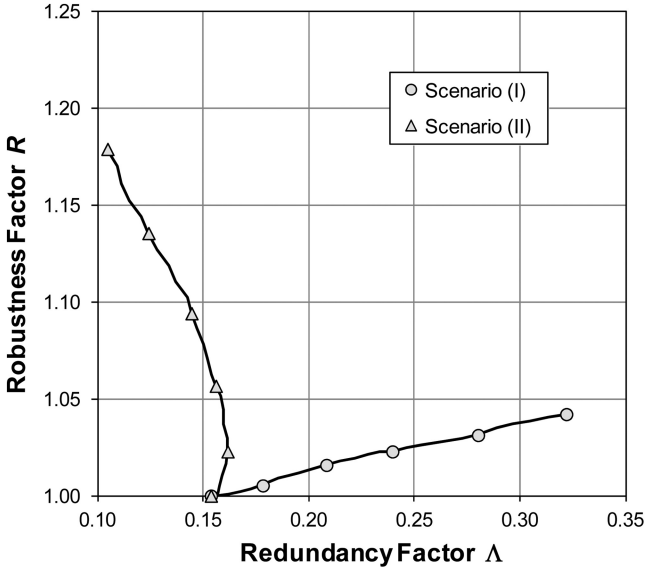

Figure 6.23 Structural robustness R vs structural redundancy Λ for scenario (I) with exposure on one side, and scenario (II) with exposure on four sides (adapted from Biondini & Frangopol 2013).

The redundancy factor $\Lambda = \Lambda(t)$ can assume values in the range [0; 1]. It is zero when there is no reserve of load carrying capacity after the first failure ($\lambda_1 = \lambda_c$), and tends to unity when the first failure load capacity is negligible with respect to the collapse load capacity ($\lambda_1 << \lambda_c$). Figure 6.22 presents the time evolution of the redundancy factor $\Lambda = \Lambda(t)$ of the frame system for the two investigated scenarios. It is noted that for cases (I) redundancy increases over time, even if the structural performance in terms of load carrying capacities decreases. This is because λ_1 has a higher deterioration rate than λ_c. On the contrary, redundancy decreases over time for case (II). Therefore, case (II) is the worst damage scenario for structural redundancy.

The results of the time-variant analyses of the frame demonstrate that robustness and redundancy are different performance indicators. In fact, as shown in Figure 6.23, opposite trends may be obtained depending on the damage scenario. For case (I), both redundancy and robustness tend to increase over time, even though the increase of robustness is small. For case (II) an opposite trend is observed, with a remarkable increase of robustness and a decrease of redundancy over time.

6.9.4 *Failure Times*

The time evolution of the limit load multipliers (Figure 6.20) indicates that the exposure scenario (II) may be critical with respect to structural collapse. For this scenario it is therefore of interest to assess the lifetimes T_1 and T_c associated to the occurrence of the first failure and collapse, respectively, as well as the elapsed time between failures $\Delta T = T_c - T_1$. The values $T_1 = 25.1$ years, $T_c = 33.2$ years, and $\Delta T = 8.1$ years are

obtained for the nominal scenario. These values indicate that after local failures a remarkable rapidity of repair may be required under severe exposures.

6.10 Role of Uncertainty and Probabilistic Analysis

Due to the uncertainties in the material and geometrical properties, in the physical models of the deterioration process, and in the mechanical and environmental stressors, a measure of time-variant structural performance of aging systems is realistically possible only in probabilistic terms (Ang & Tang 2007). This is particularly important for concrete structures exposed to corrosion since several key parameters that determine the diffusion process and corrosion initiation, such us diffusivity D and the chloride content C_0, may depend on several uncertain factors, including concrete mix, concrete cure, temperature and humidity, that are generally characterized by high coefficients of variation (Ellingwood 2005).

As an example, for the case study of the RC frame shown in Figure 6.17, the time-variant damage index $\Delta = \Delta(t)$ and the corresponding time evolution of the limit load multipliers $\lambda_1 = \lambda_1(t)$ and $\lambda_c = \lambda_c(t)$, have to be considered as random variables or processes. Therefore, a lifetime probabilistic analysis is necessary to investigate the time-variant effects of uncertainty on robustness factor R, redundancy factor Λ, and elapsed time between failures ΔT. A lifetime probabilistic analysis is then carried out by Monte Carlo simulation based on a probabilistic modeling of the diffusion process and damage propagation of concrete members exposed to corrosion.

At cross-sectional level the probabilistic model assumes as random variables the strength of both concrete f_c and steel f_{sy}, the coordinates (y_p, z_p) of each nodal point p of the member cross-section, the coordinates (y_m, z_m) and diameter $\emptyset_m$ of each steel bar m, the diffusivity coefficient D, and the steel damage rate $q_s = (C_s \Delta t_s)^{-1}$. For these variables the nominal values are assumed as mean values. The random variables are assumed uncorrelated with the probabilistic distribution and standard deviation values listed in Table 6.1.

Two limit cases are investigated by assuming the two sets of random variables associated to each column as uncorrelated or fully correlated. Figure 6.24 shows the time evolution of the probabilistic parameters of the robustness factor $R = R(t)$ and redundancy factor $\Lambda = \Lambda(t)$ based on a sample of 2000 Monte Carlo realizations of

Table 6.1 Probability distributions and standard deviation values (*nom* = nominal value).

Random Variable ($t = 0$)	Distribution Type	Standard Deviation σ
Concrete strength, f_c	Lognormal	5 MPa
Steel strength, f_{sy}	Lognormal	30 MPa
Coordinates of the nodal points, (y_p, z_p)	Normal	5 mm
Coordinates of the steel bars, (y_m, z_m)	Normal	5 mm
Diameter of the steel bars, $\emptyset_m$	Normal$^{(*)}$	$0.10\emptyset_{m,nom}$
Diffusivity, D	Normal$^{(*)}$	$0.10D_{nom}$
Steel damage rate, $q_s = (C_s \Delta t_s)^{-1}$	Normal$^{(*)}$	$0.30q_{s,nom}$

$^{(*)}$Truncated distributions with non-negative outcomes.

damage scenarios (I) and (II) for the limit case of uncorrelated random variables. These results show that the effects of uncertainty increase over time with the damage. The results also confirm that robustness and redundancy have to be regarded as different performance indicators, since different trends are obtained also in terms of uncertainty effects. In fact, the probability density functions (PDFs) of the robustness factor remain centered over the lifetime around mean values that are close to the nominal deterministic values. Conversely, the PDFs of the redundancy factor are characterized over the lifetime by mean values sensibly higher than the nominal deterministic values. This is due to the effects of randomness that, for the examined cases, emphasize the reserve of load carrying capacity $\Delta\lambda = \lambda_c - \lambda_1$ after the first local failure and lead, in this way, to a noteworthy increase on average of the lifetime structural redundancy.

Finally, Figure 6.25 shows the probability mass functions (PMFs) of the lifetimes T_1 and T_c associated to the occurrence of the first failure and collapse, respectively, as well as the elapsed time between failures $\Delta T = T_c - T_1$, for the exposure scenario (II) with uncorrelated random variables. It is noted that the effects of randomness on the reserve of load carrying capacity $\Delta\lambda$ lead to a mean value of the elapsed time ΔT

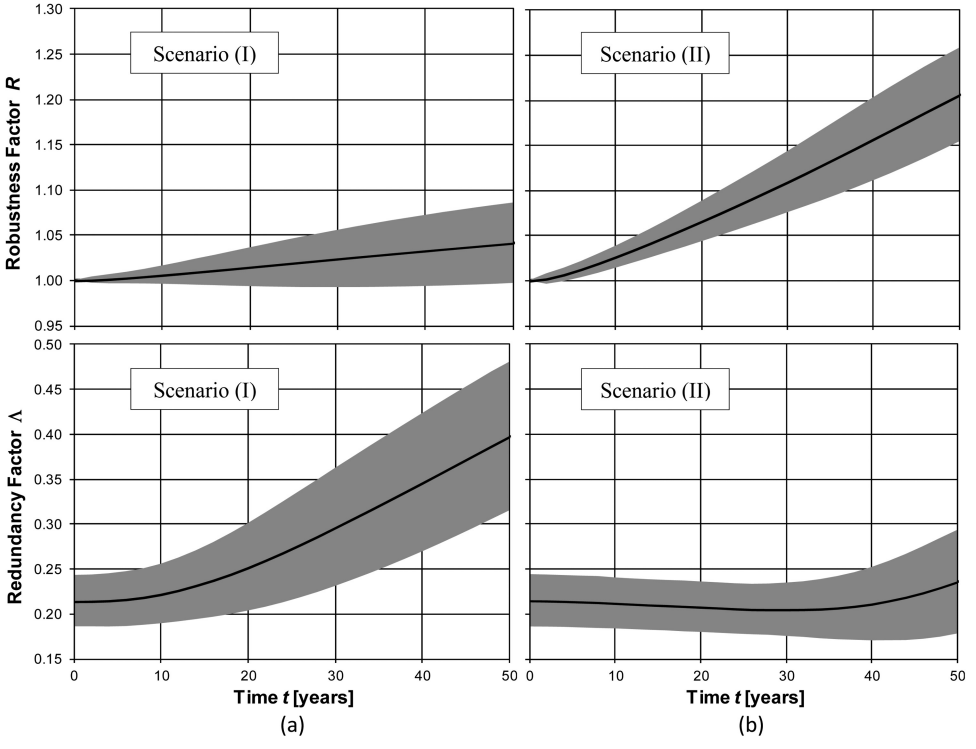

Figure 6.24 Time evolution of the probabilistic parameters of robustness factor R and redundancy factor Λ for (a) scenario (I) with exposure on one side, and (b) scenario (II) with exposure on four sides (adapted from Biondini & Frangopol 2013). The shaded region is bounded by the mean plus one standard deviation (upper bound) and the mean minus one standard deviation (lower bound).

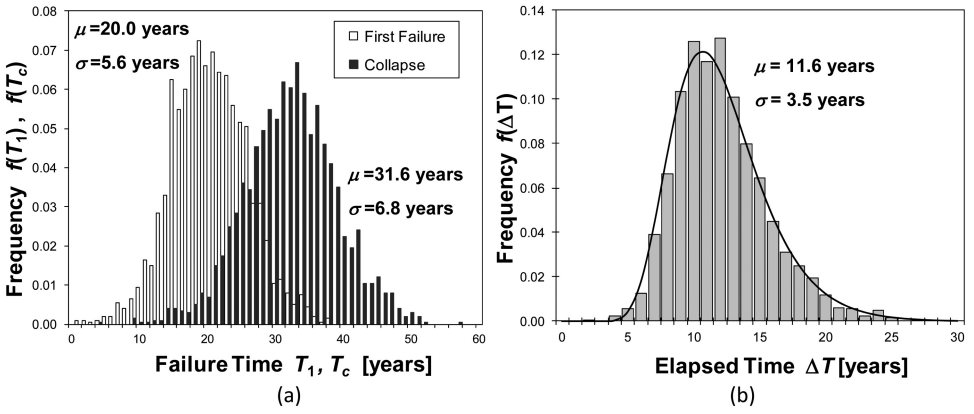

Figure 6.25 PMFs of failure times for scenario (II) with exposure on four sides (adapted from Biondini & Frangopol 2013). (a) Structural lifetimes T_1 and T_c. (b) Elapsed time between failures ΔT (PMF compared with a lognormal distribution).

higher than the nominal deterministic value. Moreover, the strong correlation between the failure loads λ_1 and λ_c is beneficial to achieve a lower variance of the elapsed time ΔT than the variance of the lifetimes T_1 or T_c.

Similar conclusions can be drawn for the limit case of fully correlated random variables. In fact, for the cases studied, correlation leads only to small changes in the variance of the investigated performance indicators and does not affect significantly the mean values. As an example, the mean and standard deviation obtained with fully correlated variables for the elapsed time ΔT are $\mu = 11.1$ years and $\sigma = 4.2$ years.

6.11 Conclusions

Redundancy of structural systems in a probabilistic context and reliability-based optimization using redundancy as a performance measure have been discussed in Frangopol & Moses (1994), Frangopol (1995), Fu & Frangopol (1990a, 1990b), Hendawi & Frangopol (1994), Okasha & Frangopol (2009, 2010a, 2010b), and Zhu & Frangopol (2013b). Recent advances in the field of structural robustness and progressive collapse of deteriorating structural systems have been presented in this chapter, with emphasis on the relationships among structural robustness, static indeterminacy, structural redundancy and failure times (Biondini & Restelli 2008, Biondini et al. 2008, Biondini 2009, Biondini & Frangopol 2010a, 2010b, 2012, 2013).

The applications demonstrated the effectiveness of the proposed measure of time-variant robustness, as well as of the damage propagation criteria, and highlighted the advantages of the presented approaches in the context of a robust structural design. In fact, the results of the applications indicated that in design of robust structures very strong members playing a disproportionate role in the structural system should be avoided, and when this is not possible, adequate solutions should be adopted to properly protect the most important members against occurrence of damage. Moreover, the degree of static indeterminacy should be adequately selected in relation to the

expected amount of damage, since an increase in the degree of static indeterminacy does not necessarily lead to an increase of structural robustness.

Measures of lifetime robustness and redundancy have been also discussed and applied to the assessment of concrete structures exposed to corrosion. The results demonstrated that robustness and redundancy are different performance indicators, which may exhibit opposite trends over time, both in deterministic and probabilistic terms, depending on the damage scenario. Moreover, the results highlighted the effectiveness of the proposed measures in comparing the robustness and redundancy associated to different systems and damage scenarios. These measures may also be used to plan eventual repair interventions and maintenance actions to protect, improve and/or restore the lifetime system performance in terms of both robustness and redundancy.

The time interval between the first local failure and structural collapse, or the elapsed time between failures, has been also investigated as an indicator of the required rapidity of the system to be repaired right after the first local failure. It has been found that after local failures a remarkable rapidity of repair may be required under severe exposure scenarios to prevent structural collapse over the lifetime. Future research should emphasize the importance of sequential failure times (Biondini 2012) and risk (Frangopol 2011, Zhu & Frangopol 2012, 2013a) in a life-cycle oriented design of robust structures under uncertainty.

Acknowledgements

The contribution of Stefano Restelli to the development of several numerical applications is gratefully acknowledged.

6.12 References

Agarwal, J., Blockley, D.I., and Woodman, N.J., (2003). Vulnerability of structural systems, *Structural Safety*, 25(3), 263–286.

Ang, A.H.-S., and Tang, W.H., (2007). *Probability concepts in engineering*. 2nd Edition, John Wiley & Sons, Hoboken, NJ, USA.

ASCE, (1968). Causes of Silver Bridge collapse studied. *ASCE Civil Engineering*, 38(12), 87.

Baker, J.W., Schubert, M., and Faber, M.H., (2008). On the assessment of robustness, *Structural Safety*, 30, 253–267.

Bertolini, L., Elsener, B., Pedeferri, P., and Polder, R., (2004). *Corrosion of steel in concrete*. Wiley-VCH, Weinheim, Germany.

Biondini, F., (2004). A three-dimensional finite beam element for multiscale damage measure and seismic analysis of concrete structures. *13th World Conference on Earthquake Engineering*, Paper No. 2963, Vancouver, B.C., Canada, August 1–6, 2004.

Biondini, F., (2009). A measure of lifetime structural robustness, *Structures Congress*, SEI/ASCE, Austin, TX, USA, April 30–May 2, 2009. In: *Structures Congress 2009*, L. Griffis, T. Helwig, M. Waggoner, M. Hoit (Eds.), ASCE, American Society of Civil Engineers.

Biondini, F., (2011). Cellular automata simulation of damage processes in concrete structures, Chapter 10 in *Soft computing methods for civil and structural engineering*, Y. Tsompanakis and B.H.V. Topping (eds.), Saxe-Coburg Publications, Stirlingshire, Scotland, pp. 229–264.

Biondini, F., (2012). Discussion of the paper: Time-variant redundancy of ship structures, by Decò, A., Frangopol, D.M., and Okasha, N.M., *Society of Naval Architects and Marine Engineers* (SNAME) *Transactions*, 119, 40.

Biondini, F., Bontempi, F., Frangopol, D.M., and Malerba, P.G., (2004). Cellular automata approach to durability analysis of concrete structures in aggressive environments, *ASCE Journal of Structural Engineering*, 130(11), 1724–1737.

Biondini, F., Bontempi, F., Frangopol, D.M., and Malerba, P.G., (2006). Probabilistic service life assessment and maintenance planning of concrete structures, *ASCE Journal of Structural Engineering*, 132(5), 810–825.

Biondini, F., and Frangopol, D.M., (2008). Probabilistic limit analysis and lifetime prediction of concrete structures, *Structure and Infrastructure Engineering*, 4(5), 399–412.

Biondini, F., and Frangopol, D.M., (2009). Lifetime reliability-based optimization of reinforced concrete cross-sections under corrosion, *Structural Safety*, Elsevier, 31, 483–489.

Biondini, F., and Frangopol, D.M., (2010a). Structural robustness and redundancy of deteriorating concrete bridges, *Fifth International Conference on Bridge Maintenance, Safety and Management* (IABMAS 2010), Philadelphia, PA, USA, July 11–15, 2010. In: *Bridge maintenance, safety, management and life-cycle optimization*, D.M. Frangopol, R. Sause, and C.S. Kusko (eds.), CRC Press, Taylor & Francis Group.

Biondini, F., and Frangopol, D.M., (2010b). Structural lifetime and elapsed time between first failure and collapse: application to an arch bridge, *Fifth International Conference on Bridge Maintenance, Safety and Management* (IABMAS 2010), Philadelphia, PA, USA, July 11–15, 2010. In: *Bridge maintenance, safety, management and life-cycle optimization*, D.M. Frangopol, R. Sause, and C.S. Kusko (eds.), CRC Press, Taylor & Francis Group.

Biondini, F., and Frangopol, D.M., (2012). Lifetime structural robustness of concrete bridge piers under corrosion, *Sixth International Conference on Bridge Maintenance, Safety and Management* (IABMAS 2012), Stresa, Italy, July 8–12, 2012. In: *Bridge maintenance, safety, management, resilience and sustainability*, F. Biondini, and D.M. Frangopol (eds.), CRC Press, Taylor & Francis Group.

Biondini, F., and Frangopol, D.M., (2013). Time effects on robustness and redundancy of deteriorating concrete structures, *11th International Conference on Structural Safety and Reliability* (ICOSSAR 2013), New York, NY, USA, June 16–20, 2013. In: *Safety, reliability, risk and life-cycle performance of structures and infrastructures*, G. Deodatis, B.R. Ellingwood, and D.M. Frangopol (eds.), CRC Press, Taylor & Francis Group.

Biondini, F., Frangopol, D.M., and Restelli, S., (2008). On structural robustness, redundancy and static indeterminacy, *Structures Congress*, SEI/ASCE, Vancouver, Canada, April 24–26, 2008. In: *Structures Congress 2008*, ASCE, American Society of Civil Engineers.

Biondini, F., and Restelli, S., (2008). Damage propagation and structural robustness, *First International Symposium on Life-Cycle Civil Engineering* (IALCCE'08), Varenna, Lake Como, Italy, June 10–14, 2008. In *Life-cycle civil engineering*, F. Biondini, and D.M. Frangopol (eds.), CRC Press, Taylor & Francis Group, 131–136.

Carper, K.L., and Smilowitz, R., (eds.) (2006). Mitigating the potential for progressive disproportionate structural collapse, Special Issue, ASCE *Journal of Performance of Constructed Facilities*, 20(4), 116 pp.

CEB, (1992). *Durable concrete structures – Design guide*, Comité Euro-international du Béton, Bulletin d'information no. 183, Thomas Telford.

Decò, A., Frangopol, D.M., and Okasha, N.M., (2011). Time-variant redundancy of ship structures, *SNAME Journal of Ship Research*, 55(3), 208–219.

Ellingwood, B.R., (2005). Risk-informed condition assessment of civil infrastructure: state of practice and research issues. *Structure and Infrastructure Engineering*, 1(1), 7–18.

Ellingwood, B.R., (2006). Mitigating risk from abnormal loads and progressive collapse. *ASCE Journal of Performance of Constructed Facilities*, 20(4), 315–323.

Ellingwood, B.R., and Dusenberry, D.O., (2005). Building design for abnormal loads and progressive collapse. *Computer-Aided Civil and Infrastructure Engineering*, 20, 194–205.

Ellingwood, B.R., and Leyendecker, E.V., (1978). Approaches for design against progressive collapse. *ASCE Journal of Structural Division*, 104(3), 413–423.

Frangopol, D.M., (1995). *Reliability-based optimum structural design*, Chapter 16 in *Probabilistic structural mechanics handbook*, C. Sundararajan (ed.), Chapman & Hall, New York, pp. 352–387.

Frangopol, D.M., (2011). Life-cycle performance, management, and optimization of structural systems under uncertainty: accomplishments and challenges, *Structure and Infrastructure Engineering*, 7(6), 389–413.

Frangopol, D.M., and Curley, J.P., (1987). Effects of damage and redundancy on structural reliability, *ASCE Journal of Structural Engineering*, 113(7), 1533–1549.

Frangopol, D.M., Iizuka, M., and Yoshida, K., (1992). Redundancy measures for design and evaluation of structural systems, *ASME Journal of Offshore Mechanics and Arctic Engineering*, 114(4), 285–290.

Frangopol, D.M., and Klisinski, M., (1989). Weight-strength-redundancy interaction in optimum design of three-dimensional brittle-ductile trusses, *Computers and Structures*, 31(5), 775–787.

Frangopol, D.M., and Moses, F., (1994). *Reliability-based structural optimization*, Chapter 13 in *Advances in design optimization*, H. Adeli (ed.), Chapman & Hall, London, pp. 492–570.

Frangopol, D.M., and Nakib, R., (1991). Redundancy in highway bridges, *AISC Engineering Journal*, 28(1), 45–50.

Frangopol, D.M., and Saydam, D., (2013). *Structural performance indicators for bridges*, Chapter 9 in *Bridge engineering handbook – Vol. 1 Fundamentals*, W.-F. Chen and L. Duan (eds.), CRC Press / Taylor & Francis, 2nd Edition, pp. 185–205.

Fu, G., and Frangopol, D.M., (1990a). Reliability-based vector optimization of structural systems, *ASCE Journal of Structural Engineering*, 116(8), 2143–2161.

Fu, G., and Frangopol, D.M., (1990b). Balancing weight, system reliability and redundancy in a multiobjective optimization framework. *Structural Safety*, 7(2–4), 165–175.

Ghosn, M., Moses, F., and Frangopol, D.M., (2010). Redundancy and robustness of highway bridge superstructures and substructures, *Structure and Infrastructure Engineering*, 6(1–2), 257–278.

Glicksman, M.E., (2000). *Diffusion in solids*, John Wiley and Sons.

Griffiths, H., Pugsley, A.G., and Saunders, O., (1968). *Report of the inquiry into the collapse of flats at Ronan Point, Canning Town*. Great Britain, Ministry of Housing and Local Government, Her Majesty's Stationery Office, London.

Hendawi, S., and Frangopol, D.M., (1994). System reliability and redundancy in structural design and evaluation. *Structural Safety*, 16, (1–2), 47–71.

Liu, T., and Weyers, R.W., (1998). Modeling the dynamic corrosion process in chloride contaminated structures. *Cement and Concrete Research*, 28(3), 365–379.

Lu, Z., Yu Y., Woodman, N.J., and Blockley, D.I., (1999). A theory of structural vulnerability. *The structural engineer*, 77(18), 17–24.

NTSB, (1983). *Collapse of suspended span of Route 95 highway bridge over the Mianus River Greenwich, Connecticut June, 28, 1983*. Highway Accident Report, National Transportation Safety Board, Washington D.C.

Okasha, N.M., and Frangopol, D.M., (2009). Lifetime-oriented multi-objective optimization of structural maintenance, considering system reliability, redundancy, and life-cycle cost using GA, *Structural Safety*, 31(6), 460–474.

Okasha, N.M., and Frangopol, D.M., (2010a). Time-variant redundancy of structural systems, *Structure and Infrastructure Engineering*, 6, 279–301.

Okasha, N.M., and Frangopol, D.M., (2010b). Redundancy of structural systems with and without maintenance: An approach based on lifetime functions, *Reliability Engineering & System Safety*, 95(5), 520–533.

Pastore, T., and Pedeferri, P., (1994). La corrosione e la protezione delle opere metalliche esposte all'atmosfera, *L'edilizia*, December, 1994, 75–92 (In Italian).

Powell, G., (2009). Disproportionate collapse: The futility of using nonlinear analysis, *Structures Congress*, SEI/ASCE, Austin, TX, USA, April 30–May 2, 2009. In: *Structures Congress 2009*, L. Griffis, T. Helwig, M. Waggoner, M. Hoit (Eds.), ASCE, American Society of Civil Engineers.

Saydam, D., and Frangopol, D.M., (2011). Time-dependent performance indicators of damaged bridge superstructures, *Engineering Structures*, 33(9), 2458–2471.

Starossek, U., (2008). Collapse resistance and robustness of bridges, *Fourth International Conference on Bridge Maintenance, Safety and Management* (IABMAS'08), Seoul, Korea, July 13–17. In: *Bridge maintenance, safety, management, health monitoring and informatics*, H.-M. Koh, and D.M. Frangopol (eds.), CRC Press, Taylor & Francis Group.

Starossek, U., (2009). *Progressive collapse of structures*. Thomas Telford Publishing, London, UK.

Starossek, U., Haberland, M., (2011). Approaches to measures of structural robustness, *Structure and Infrastructure Engineering*, 7(7–8), 625–631.

Stewart, M.G., (2009). Mechanical behaviour of pitting corrosion of flexural and shear reinforcement and its effect on structural reliability of corroding RC beams, *Structural Safety*, 31, 19–30.

Taylor, D.A., (1975). Progressive collapse. *Canadian Journal of Civil Engineering*, 2(4), 517–529.

Thoft-Christensen, P., (1998). Assessment of the reliability profiles for concrete bridges. *Engineering Structures*, 20(11), 1004–1009.

Zhu, B., and Frangopol, D.M., (2012). Reliability, redundancy and risk as performance indicators of structural systems during their life-cycle, *Engineering Structures*, 41, 34–49.

Zhu, B., and Frangopol, D.M., (2013a). Risk-based approach for optimum maintenance of bridges under traffic and earthquake loads, *ASCE Journal of Structural Engineering*, 139(3), 422–434.

Zhu, B., and Frangopol, D.M., (2013b). Incorporation of SHM data on load effects in the reliability and redundancy assessment of ships using Bayesian updating, *Structural Health Monitoring*, 12(4), 377–392.